Human CD49a+ lung NK cell cytotoxicity in response to Influenza A Virus

Grace E. Cooper[1], Kristoffer Ostridge[1], Salim I. Khakoo[1], Tom Wilkinson[1], Karl J. Staples[1*]

[1]Faculty of Medicine, University of Southampton, United Kingdom

Submitted to Journal:
Frontiers in Immunology

Specialty Section:
NK and Innate Lymphoid Cell Biology

Article type:
Original Research Article

Manuscript ID:
395662

Received on:
10 May 2018

Revised on:
03 Jul 2018

Frontiers website link:
www.frontiersin.org

Conflict of interest statement

The authors declare a potential conflict of interest and state it below

KS and TW have applied for a patent for the explant infection model (PCT/GB2010/050821 "Ex Vivo Modelling of Therapeutic Interventions"). The report funding from GSK Biologicals SA and AstraZeneca outside of the submitted work. GC, KO and SK have no potential conflict of interest to declare.

Author contribution statement

Data acquisition, analysis and interpretation was provided by GC, KO and KS. All authors contributed to the drafting of manuscript for important intellectual content and manuscript conception and design

Keywords

NK cells, Human lung, viral infection, Cytotoxicity, CD49a, Influenza A virus

Abstract

Word count: 294

Influenza A virus (IAV) is a major global public health burden due to its routine evasion of immunisation strategies. Natural Killer (NK) cells are innate cytotoxic cells with important antiviral activity in the human body, yet the function of these cells in the control of IAV infection is unclear. The aim of this study was to determine the role of lung NK cell cytotoxic responses to IAV. Human lung explants were infected ex vivo with IAV and lung NK cell activation was analysed by flow cytometry. Cytotoxic responses of NK cell subsets against IAV-infected macrophages were measured by flow cytometry and ELISA. Despite reports of hypofunctionality in the pulmonary environment, human lung-associated NK cells responded rapidly to ex vivo IAV infection, with upregulation of surface CD107a 24 h post-infection. The lung NK cell phenotype is similar in maturity and differentiation to NK cells of the peripheral blood but a unique CD56brightCD49a+CD103+CD69+ NK cell population was identified in the lung, indicating NK cell residency within this organ. In response to ex vivo IAV infection a greater proportion of resident CD56brightCD49a+ NK cells expressed surface CD107a compared to CD56brightCD49a- NK cells, suggesting a hyperfunctional NK cell population may be present within human lung tissue and could be the result of innate immunological training. Furthermore NK cells provided significant anti-viral, cytotoxic activity following contact with influenza infected cells, including the production and release of IFN-γ and Granzyme-B resulting in macrophage cell death. These results suggest that a resident, memory NK cell population are present in the human lung and may provide early and important control of viral infection. A greater understanding of this resident mucosal population may provide further insight into the role of these cells in controlling viral infection and generating appropriate adaptive immunity to IAV.

Funding statement

This work was part funded by the BMA HC Roscoe Award 2013 to KS and TW. GC was funded by a 4 year MRC PhD studentship.

Ethics statements

(Authors are required to state the ethical considerations of their study in the manuscript, including for cases where the study was exempt from ethical approval procedures)

Does the study presented in the manuscript involve human or animal subjects: Yes

Please provide the complete ethics statement for your manuscript. Note that the statement will be directly added to the manuscript file for peer-review, and should include the following information:

- Full name of the ethics committee that approved the study
- Consent procedure used for human participants or for animal owners
- Any additional considerations of the study in cases where vulnerable populations were involved, for example minors, persons with disabilities or endangered animal species

As per the Frontiers authors guidelines, you are required to use the following format for statements involving human subjects:
This study was carried out in accordance with the recommendations of [name of guidelines], [name of committee]. The protocol was approved by the [name of committee]. All subjects gave written informed consent in accordance with the Declaration of Helsinki.
For statements involving animal subjects, please use:
This study was carried out in accordance with the recommendations of 'name of guidelines, name of committee'. The protocol was approved by the 'name of committee'.

If the study was exempt from one or more of the above requirements, please provide a statement with the reason for the exemption(s).
Ensure that your statement is phrased in a complete way, with clear and concise sentences.

This study was approved by Southampton and South West Hampshire Research Ethics Committees (13/SC/0416 for healthy control group, 09/H0504/109 for resection and blood donors, 15/SC/0528 for age comparison). All participants provided written informed consent in accordance with the Declaration of Helsinki.

Human CD49a+ lung NK cell cytotoxicity in response to Influenza A Virus

Grace E Cooper (MRes)[1] Kristoffer Ostridge (PhD)[1,2] Salim Khakoo (MD)[1] Tom M.A. Wilkinson (PhD)[1,2,3] Karl J. Staples (PhD)[1,3*]

1 Clinical & Experimental Sciences, University of Southampton Faculty of Medicine, Sir Henry Wellcome Laboratories, Southampton General Hospital, Tremona Road, Southampton, SO16 6YD

2 Southampton NIHR Respiratory Biomedical Research Unit, Southampton General Hospital, Tremona Road, Southampton, SO16 6YD

3 Wessex Investigational Sciences Hub, University of Southampton Faculty of Medicine, Southampton General Hospital, Tremona Road, Southampton, SO16 6YD

***Correspondence:** Dr Karl J. Staples (ORCID: 0000-0003-3844-6457), Clinical and Experimental Sciences, University of Southampton Faculty of Medicine, Sir Henry Wellcome Laboratories, Mailpoint 810, Southampton General Hospital, Tremona Road, Southampton, SO16 6YD, UK. Tel: +44 23 8120 6397 Fax: +44 23 8070 1771 Email: k.staples@southampton.ac.uk

Keywords: NK cells, human lung, viral infection, cytotoxicity, CD49a

Abstract

Influenza A virus (IAV) is a major global public health burden due to its routine evasion of immunisation strategies. Natural Killer (NK) cells are innate cytotoxic cells with important antiviral activity in the human body, yet the function of these cells in the control of IAV infection is unclear. The aim of this study was to determine the role of lung NK cell cytotoxic responses to IAV. Human lung explants were infected *ex vivo* with IAV and lung NK cell activation was analysed by flow cytometry. Cytotoxic responses of NK cell subsets against IAV-infected macrophages were measured by flow cytometry and ELISA. Despite reports of hypofunctionality in the pulmonary environment, human lung-associated NK cells responded rapidly to *ex vivo* IAV infection, with upregulation of surface CD107a 24 h post-infection. The lung NK cell phenotype is similar in maturity and differentiation to NK cells of the peripheral blood but a unique $CD56^{bright}$CD49a+CD103+CD69+ NK cell population was identified in the lung, indicating NK cell residency within this organ. In response to *ex vivo* IAV infection a greater proportion of resident $CD56^{bright}$CD49a+ NK cells expressed surface CD107a compared to $CD56^{bright}$CD49a- NK cells, suggesting a hyperfunctional NK cell population may be present within human lung tissue and could be the result of innate immunological training. Furthermore NK cells provided significant anti-viral, cytotoxic activity following contact with influenza infected cells, including the production and release of IFN-γ and Granzyme-B resulting in macrophage cell death. These results suggest that a resident, trained NK cell population are present in the human lung and may provide early and important control of viral infection. A greater understanding of this resident mucosal population may provide further insight into the role of these cells in controlling viral infection and generating appropriate adaptive immunity to IAV.

Word count: 4244

Figure count: 13

1 Introduction

Influenza A Virus (IAV) is a ssRNA virus of the Orthomyxoviridae family causing acute infection of the upper and lower respiratory tract (Taubenberger and Kash 2010). IAV infection remains a global public health burden with 3-5 million cases of severe illness and 500,000 deaths worldwide, annually (Stohr 2002). Vaccination is currently the best method of controlling viral transmission, however annual influenza vaccines are limited in efficacy due to rapid viral evolution, time required for production and ineffectiveness in high-risk groups (Greenberg and Piedra 2004, Mossad 2016). Improving the current immunization strategies requires a more advanced understanding of both innate and adaptive human immunity to influenza virus (Krammer and Palese 2015).

The lungs are one of the largest reservoirs of NK cells in the body, yet the function of these cells in pulmonary viral infection is poorly understood (Romagnani *et al.* 2007, Wong *et al.* 2016). Natural Killer (NK) cells are antiviral lymphocytes essential to the control of human pathogens such as Hepatitis C Virus, Cytomegalovirus and Human Immunodeficiency Virus (Vivier *et al.* 2008, Yoon *et al.* 2016). NK cells aid viral clearance through secretion of pro-inflammatory cytokines such as IFN-γ as well as cytotoxic granules and engagement of death receptors, which stimulate target cell apoptosis (Vivier *et al.* 2008). Different subpopulations of human NK cells can be identified through high and low expression of CD56, and these populations of NK cells have been ascribed different functions. $CD56^{bright}$ NK cells are thought to be predominantly cytokine producing whilst $CD56^{dim}$ NK cells represent the canonical cytotoxic NK cell, however these functional outputs appear dependent on the type of *in vitro* stimulation and the role of these NK cell subtypes within the human body remain largely unexplored (Nagler *et al.* 1989, Cooper *et al.* 2001, Jacobs *et al.* 2001, Moretta 2010, De Maria *et al.* 2011).

NK cells recognize virally infected cells through the integration of signaling from activatory and inhibitory germline encoded receptors on the NK cell surface (Vivier *et al.* 2004). *In vitro* binding studies have shown that the activatory NK cell receptors NKG2D and NKp46, and inhibitory KIR2DL2 NK cell receptor bind influenza-infected cells (Mandelboim *et al.* 2001, Draghi *et al.* 2007, Achdout *et al.* 2008). Furthermore, strong IFN-γ responses are observed in the NK cells of the peripheral blood following influenza vaccination (He *et al.* 2004, He *et al.* 2006, Long *et al.* 2008, Jost *et al.* 2011). The majority of mouse models of influenza infection implicate a protective role for NK cells during infection (Stein-Streilein and Guffee 1986, Gazit *et al.* 2006, Nogusa *et al.* 2008, Kumar *et al.* 2013, Zhou *et al.* 2016). Indeed *Ncr1*-/- (NKp46) knockout in the mouse results in lethal influenza infection (Gazit *et al.* 2006). However, in most high dose infection models murine NK cells appear to play a detrimental role, contributing to influenza pathogenesis (Abdul-Careem *et al.* 2012, Zhou *et al.* 2013). This may suggest there is a delicate balance between protective and destructive NK cell activation during IAV infection. But due to differences in influenza strain, dose and genetic background of the mice it is difficult to delineate what role NK cells may play in murine models of influenza infection.

The majority of studies investigating the human NK cell responses to influenza utilise peripheral blood NK cells (He *et al.* 2004, He *et al.* 2006, Draghi *et al.* 2007, Long *et al.* 2008, Jost *et al.* 2011). However, organ resident NK cell populations have recently been identified in the liver, uterus and secondary lymphoid tissue, with resident populations expressing CD103, CD69 and CD49a (Koopman *et al.* 2003, Marquardt *et al.* 2015, Björkström *et al.* 2016, Lugthart *et al.* 2016, Montaldo *et al.* 2016).

Phenotypically different from the blood, these populations have been linked to NK cell memory and may possess different functionality as a result of "training" by their environment (Peng and Tian 2017). Lung NK cell residency has been disputed, with lung NK cells often described as hypofunctional (Robinson *et al.* 1984, Michel *et al.* 2012, Wang *et al.* 2012, Marquardt *et al.* 2017). However, there is some evidence that NK cell memory can be generated to respiratory virus, as murine influenza infection induced liver CD49a+ NK cells that are protective against influenza infection (Li *et al.* 2017). Furthermore, influenza vaccination results in a more potent NK cell response to influenza in human peripheral blood mononuclear cells (PBMCs) (Dou *et al.* 2015).

The contribution of NK cells to pulmonary health and disease is poorly understood in humans and how NK cells may respond to influenza infection has not been characterized in a model effectively recapitulating human infection. The aim of this study was therefore to investigate the role of human lung NK cells in early influenza control using our previously characterized lung explant model of influenza infection (Nicholas *et al.* 2015, Staples *et al.* 2015, McKendry *et al.* 2016).

2 Materials & methods

2.1 Volunteer recruitment

Lung tissue distal from tumour sites and peripheral blood was obtained from lobectomy patients. Blood was also obtained from healthy human volunteers. All studies were approved by Southampton and South West Hampshire Research Ethics Committees (13/SC/0416 for healthy control group, 09/H0504/109 for resection and blood donors, 15/SC/0528 for age comparison). All participants provided written informed consent.

2.2 Preparation of lung tissue and explant infection

Lung tissue explants were prepared as previously described and infected with X31 (H3N2) Influenza A Virus (Virapur) as previously described (McKendry et al. 2015, Staples et al. 2015). Briefly, lung tissue explants were cut into 4-6mm^2 pieces with 6 fragments/well and washed thoroughly with cold RPMI. The lung explants were then rested for 16h in complete RPMI (RPMI with 10% FCS, 2mg/mL L-glutamine, 0.05IU/mL Penicillin, 50µg/mL Streptomycin and 0.25µg/mL Amphotericin B (Sigma)) to remove contaminant blood. For NK cell phenotyping the lung tissue was digested in 0.5mg/mL collagenase, filtered through a 0.7µm filter and mononuclear cells isolated by density gradient centrifugation over a Ficoll-paque layer. Cells isolated from the buffy coat were then stained for flow cytometry. For IAV infection of lung explants, lung fragments were washed in PBS and infected with 200,000 pfu/ml live or UV-irradiated X31 (H3N2) Influenza A Virus (Virapur) following rest (Nicholas *et al.* 2015, Cooper *et al.* 2016). UV-irradiated X31 was created by exposing live X31 to UV light for 2 h on ice. 2 hpi extracellular virus was removed by washing in PBS and explants cultured in fresh media for a further 22h, or for stated time point. X31 replication was detected through intracellular viral NP1 expression. In addition lung explants were alternatively treated with Phorbol myristate acetate and Ionomycin (PMA/I – 1.34 µM and 81 nM respectively). After infection NK cells were dispersed from tissue using 0.5 mg/ml collagenase, the digest filtered and cells stained for flow cytometry.

A median of 410,676 ± 153,226 CD45+ leukocytes were isolated per resection sample, according to flow cytometry analysis. The median total events in the NK cell gate was 10,011 ±9,073 and a

minimum value of 2,760 (N=8). For the rarer CD56^{bright} CD49a+ NK cells the median number of events was 940 ± 194 and a minimum value of 130; a cut off of a minimum 100 events in this gate was required to be included in the analysis (N=8). The same cut off was used in the functional studies of the CD56^{bright}CD49a+ population. The median number of events for CD56^{bright}CD49a+ NK cells in the X31-infected explant was 1,035 ± and a minimum value of 164 (N=5). This was also typical of the untreated and UV-irradiated X31 treated explant tissue.

2.3 Blood NK cell and monocyte isolation & differentiation

Human PBMCs were isolated from heparinised blood of healthy volunteers or from cancer resection donors. Blood was diluted 1:1 with PBS and mononuclear cells isolated by density gradient centrifugation on Ficoll-Paque (GE Healthcare). Monocytes were isolated from PBMC by CD14 positive Magnetic-associated cell sorting (MACS) (Miltenyi Biotec). Monocytes were seeded at 500 000 cells/well (1 x 10^6 cells/ml) and differentiated into monocyte-derived macrophages (MDMs) over 12 days in complete RMPI with 2 ng/ml GM-CSF, as described previously (Staples *et al.* 2012). Autologous NK cells were isolated from the CD14-depleted MACS filtrate by negative selection with an NK cell isolation kit (Miltenyi) according to manufacturer's instructions. Purified NK cells (94.28% CD3-CD56+, N=5) were frozen in FCS containing 10% DMSO (Sigma) until use.

2.4 Macrophage infection and co-culture with NK cells

MDM infection was performed as previously described (Staples *et al.* 2015). MDMs were treated with 500 pfu/mL of live or UV-irradiated X31 virus for 2h, before removal of extracellular virus by washing with PBS and incubation for a further 22h. UV-irradiated X31 was created by exposing live X31 to UV light for 2 h on ice. After 24 h, autologous NK cells were thawed and cultured with untreated or infected MDMs for 6 h at an E:T of 1:5. This E:T was chosen following testing of a range of E:T of NK cells to X31-infected MDMs, as shown in Supplementary Figure 1 and was chosen for the optimal detection of NK cell IFN-γ production. NK cell degranulation, IFN-γ and Gzm-B production and MDM viability were measured by flow cytometry. Adherent MDMs were collected for flow cytometry with non-enzymatic cell dissociation solution (Sigma). To measure the accumulation of intracellular molecules 2 µM Monensin (eBiosciences) was added into the co-culture 1 h after the addition of NK cells. Physical contact between MDMs and NK cells was prevented through culturing in a transwell system with NK cells in the top compartment (Costar). HLA class I binding was blocked through incubation of 20 µg/mL αHLA-A/B/C (W6/32; Biolegend) with MDM 20min prior to addition of NK cells.

2.5 Flow cytometry

Flow cytometry was performed as previously described, all steps were performed at 4°C for 30min, unless otherwise stated (Staples *et al.* 2015). Cell viability was assessed by staining with Zombie Violet Fixable Viability Kit (Biolegend) in PBS. Surface marker staining was performed in 2mM EDTA and 0.5% Bovine Serum Albumin (FACS buffer) with 2mg/mL human IgG (Sigma). Cellular surface markers were stained with the following antibodies; 5µL αCD3-PerCP (UCHT1), 5µL αCD56-PECy7 (HCD56), 5µL αCD57-PacificBlue (HCD57), 5µL αCD103-APC (Ber-ACT8), 5µL αCD69-BV421 (FN50), 5µL αCD107a-BV510 (H4A3) (Biolegend), 5µL αCD45-BV510 (HI30), 5µL αCD16-FITC (3G8), 20µL αCD49a-PE (SR84), 20µL αCD158b-PE (CH-L), (BD Biosciences) and with corresponding isotype controls; Mouse IgG1-PerCP, IgG1-PECy7, IgG2b-PE, IgM-Pacific Blue, IgG1-APC, IgG1-BV421 (Biolegend) Mouse IgG1-BV510, IgG1-FITC, IgG1-PE (BD Biosciences).

Macrophages and epithelia were stained with, 5µL αHLA-DR-APC-Cy7 (L243) and 20µL αEpCAM-PerCP-Cy5.5 (EBA-1), 5µL αHLA-ABC-PE (W6/32) (BD Biosciences). Corresponding isotype controls not previously stated included Mouse IgG2a-APC-Cy7 (BD Biosciences) and IgG2a-PE (Life Tech). Cells were then fixed and permeabilised with Cytofix/Cytoperm (BD Biosciences, Oxford, UK) for 20min before intracellular staining. Intracellular staining was performed in 1 x Permwash (BD Biosciences) in FACS staining buffer. Intracellular markers were assessed with 2µL α-nucleoprotein (NP)-1-FITC (ab20921) (Abcam), 5µL αIFN-γ-PerCP-Cy5.5 (4S.B3) or 5µL αGzm-B-APC (QA16A02) (Biolegend). Flow cytometric analysis was performed on a FACSAria using FACSDiva software v5.0.3 (BD Biosciences) and FlowJo v10 (TreeStar). The t-SNE algorithm was applied within FlowJo v10 for 1000 iterations to produce 2D projections of the data using a perplexity value of 20. FCS files from the lung and matched blood, or lung only, were downsampled to 300 or 600 cells respectively.

2.6 ELISA

IFN-γ ELISA MAX (Biolegend), and Granzyme B duoset ELISA (R&D Systems) were all carried out according to the manufacturer's protocol.

2.7 Statistics

Statistical analyses were performed using either a Chi-squared test, Fisher's test, Wilcoxon's matched-pairs signed-rank test, Mann-Whitney U test, Kruskal-Wallis or Friedman test with Dunn's multiple comparison testing as appropriate (GraphPad Prism v7.0, GraphPad Software Inc., San Diego, USA). Data are expressed as medians. Results were considered significant if $P<0.05$.

3 Results

3.1 NK cells are present at high frequencies in human lung parenchyma

NK cells were isolated from human lung parenchyma, matched peripheral blood and peripheral blood from healthy controls. NK cells were defined as CD45+CD3-CD56+ cells by flow cytometry and made up a median of 18.55% ±14.98 of CD45+ lymphocytes isolated from the human lung parenchyma (N=17, Figure 1). $CD56^{bright}CD16$-, $CD56^{dim}CD16$+ and $CD56^{dim}CD16$- NK cells were all identified in lung and blood with $CD56^{dim}CD16$+ and $CD56^{dim}CD16$- found in similar proportions between the lungs and peripheral blood (P=0.83 and P=0.50, Figure 1 C, D and E). As described by Marquardt *et al* 2017, the majority of lung-associated NK cells are canonical cytotoxic $CD56^{dim}CD16$+ cells (Marquardt *et al.* 2017). However, we observed an increased proportion of $CD56^{bright}$ NK cells in the lungs compared to matched peripheral blood (8.6% vs 3.3%, P=0.0049, Figure 1C). Furthermore, fewer $CD56^{dim}CD16$+ NK cells (P=0.0012) and a greater proportion of $CD56^{dim}CD16$- NK cells were isolated from the blood of cancer resection patients compared to healthy control blood.

These differences in the NK cell subpopulations may reflect differences in the cohort age and smoking status between healthy controls and donors undergoing resection surgery, as shown in Table 1. To assess the effect of age on NK cell subpopulations of the blood, the proportions of CD56bright and CD56dim NK cells were analysed from the blood of healthy controls aged above and below 40 (donor demographics shown in Table 2). However, no differences were observed in the peripheral NK cell subpopulations of these two cohorts (Figure 2)

To evaluate the maturity of lung NK cells, the expression of CD57 and CD158b (KIR2DL2/L3/S2) were analysed on lung and blood NK cells. CD57 is expressed in the late stages of NK cell differentiation and is associated with increased NK cell functionality (Bjorkstrom *et al.* 2010, Lopez-Verges *et al.* 2010). KIR expression also increases during NK cell maturation, as NK cells gain cytotoxic function (Freud *et al.* 2006, Poli *et al.* 2009). Although CD158b does not evaluate the expression of all KIR, which vary across individuals, it represents KIR from both haplotypes A and B (Uhrberg *et al.* 2002). Individuals with haplotype A typically possess KIR alleles with a more inhibitory role than the KIR haplotype B, which has a more activating effect on NK cell function (Middleton and Gonzelez 2010). Both CD57 and CD158b were expressed equivalently between lung and matched peripheral blood (Figure 3 A and C, P=0.91 and P=0.07 respectively). Furthermore, no significant differences were observed in the expression of either CD57 or CD158b on $CD56^{bright}$ or $CD56^{dim}$ NK cell subpopulations (Figure 3 B and D). To investigate whether the differentiation state of CD158b positive and negative NK cells were different between matched blood and lung, the co-expression of CD57 and CD158b were analysed, as shown in Figure 3E and F, however no significant differences were observed (P>0.9999 for each analysis of CD57+CD158b-, CD57-CD158b+, double positive and double negative NK cells). In addition, NKG2C, an activating receptor associated with CMV immunity and memory response was not found to be differentially expressed between blood and lung (Figure 3 G and 3H) (Guma *et al.* 2006, Schlums *et al.* 2015). Thus lung NK cells appear to mirror the phenotype of the peripheral blood, as highly mature and terminally differentiated NK cells. These results confirm reports by Marquardt *et al.* 2007 and other studies from the human lung (Freeman *et al.* 2014, Marquardt *et al.* 2017).

3.2 Distinct CD49a+CD103+CD69+ NK cell populations are present in the lung parenchyma

NK cells isolated from the lungs and peripheral blood appear phenotypically similar in terms of their CD16, CD57, CD158b and NKG2C expression (Figures 1 and 3), however a distinct CD49a+ NK cell population was identified from the lung parenchyma, which was not found in the circulation (Figure 4). CD49a+ NK cells made up 13.3% ±11 of the total lung-associated NK cell population and were primarily $CD56^{bright}$CD16- and $CD56^{dim}$CD16- NK cells (42.2% and 27.3% respectively, Figure 4A and 4B). Negligible amounts of CD49a were detected on $CD56^{dim}$CD16+ NK cells. Other putative markers of residency including CD69 and CD103 were also identified in the lung parenchyma with 3.65% ±7.65 of lung NK cells expressing CD103+, a marker also not found in the blood (P=0.016, Figure 4C and D). The expression of CD103 mirrored that of CD49a, with most CD103 expressed on $CD56^{bright}$ and $CD56^{dim}$CD16- NK cells. Although CD69 was not expressed differently between blood and lung at the whole NK cell level (P=0.85), $CD56^{bright}$ lung NK cells expressed greater levels of CD69 compared to the blood (P=0.0015, Figure 4E and F). CD69 was expressed at similar levels by lung $CD56^{dim}$CD16+ and $CD56^{dim}$CD16- NK cells (P=0.33 and 0.18).

The co-expression of CD49a, CD69 and CD103 on lung and blood $CD56^{bright}$ NK cells was analysed as shown in Figure 5A and 5B and visualized in t-SNE plots (Figure 5C and D). Lung $CD56^{bright}$ NK cells clustered together and appeared distinct to $CD56^{bright}$ of matched peripheral blood (Figure 5C). Analysis of CD49a, CD69 and CD103 expression on lung NK cells suggests that the CD56bright population consists of NK cells that are single positive, double positive and triple positive for these markers (Figure 6D and F). Whereas only CD69 could be identified in the peripheral blood CD56bright population (Figure 5B, 5G and 4E). Single positive CD49a+ NK cells were positioned together with

triple and double positive populations within the t-SNE analysis, however CD56^{bright} NK cells that were single positive for CD69 appeared more distinct, as did NK cells negative for all tested residency markers (Figure 5D). CD69 and CD103 were both strongly co-expressed on CD49a+CD56^{bright} NK cells, indicating that this population may be resident within the lungs (Figure 5E). One of the largest populations of lung CD56^{bright} NK cells were CD49a+CD69+CD103+, which made up 20.9% ±12.66 of the CD56^{bright} lung NK cell population Figure 5E and F).

3.3 Ex vivo IAV (H3N2) infects the macrophages and epithelia of human lung explants

NK cells make up a substantial proportion of the lung CD45+ leukocytes (18.55% ±14.98) and their response to respiratory infection may have important implications for human disease. Furthermore lung-resident NK cell populations such as the CD49a+ NK cells may be shaped by insult and homeostasis within the lung microenvironment. Therefore, to understand the functional relevance of the lung NK cell phenotypes described here, the response of lung NK cells to IAV infection were characterised in human lung parenchyma. The lung explants were infected with 200,000 pfu/mL UV-irradiated or live X31 IAV for 2h before removal of extracellular virus and further culture for a further 22h. Cells were defined as infected when viral nucleoprotein (NP)-1 was detected (Figure 6A and 6B). UV-irradiated IAV was not found to replicate within the lung tissue, as determined by NP1 expression, indicating that the virus is no longer viable (Figure 6C and F). In this model 7.07% of lung epithelia (defined as CD45-EpCAM+ cells, Figure 6A and B) and 22.3% of macrophages (defined as CD45+HLA-DR+ cells, Figure 6D and E) were infected with IAV. Both the airway epithelium and macrophages increased expression of cell surface HLA class I, a key molecule controlling NK cell activation, in response to infection (Epithelium p=0.0078, Macrophage p=0.0020, Figure 6 G and H).

3.4 NK cells activate in response to influenza infection of human lung explant

NK cells were strongly activated 24h post influenza infection (hpi), with a two-fold increase in surface CD107a when compared to UV-irradiated X31 treated explant (Figure 7B, P=0.047). NK cell degranulation was not dominated by any particular subpopulation as CD56^{bright}, CD56^{dim}CD16+ and CD56^{dim}CD16- NK cells all expressed similar levels of CD107a in X31-infected tissue (Figure 5C). There was a slight trend towards increased NK cell degranulation when MDMs were exposed to UV-irradiated virus compare to uninfected (NT) controls (P=0.094, Figure 7B). Since multiple influenza infections may be experienced throughout life we hypothesised that prior exposure to influenza may have resulted in increased functionality of the lung CD49a+ NK cell populations (Figure 4). To investigate this, the degranulation of CD56^{bright}CD49a+ NK cells in response to X31 infection was compared to CD56^{bright}CD49a- NK cells. As shown in Figure 7D the degranulation of CD56^{bright}CD49a+ NK cells was increased relative to CD56^{bright}CD49a- NK cells (12.2% vs 19.2%, P=0.031) 24hpi, indicating that these NK cells may be more responsive to influenza infection. Furthermore, CD56^{bright}CD49a+ and CD49a- NK cells were not differentially activated when explants were treated with PMA/I, indicating that the total potential of CD56^{bright}CD49a+ NK cells is similar to CD56^{bright}CD49a- NK cells. Thus this may be a virus-specific activation of CD49a+ NK cells. CD49a was also found to be expressed on CD56^{dim}CD16- NK cells, however no difference in the response to virus was observed between CD49a+ and CD49a- CD56^{dim}CD16- NK cell (Figure 7E).

Increased CD107a on the NK cells surface was mirrored by increased extracellular Granzyme-B and IFN-γ (Figure 7 F and G, P=0.0078 and P=0.0039 respectively). Granzyme-B and IFN-γ are key

molecules associated with NK cell activation and were found to rise over a similar time-course with NK cell degranulation (Figure 8). Taken together the results presented here indicate that lung-associated NK cells activate rapidly as a result of *ex vivo* IAV infection. To further test if this was a discrete effect of NK cells or related to other cell types present in the explant model, we investigated the functional effects of NK cell activation in direct co-culture with infected macrophages.

3.5 NK cells are cytotoxic towards IAV infected MDMs

Airway macrophages were a target of H3N2 IAV infection in the explant lung model and have been shown to be critical to influenza control in mice (Kim *et al.* 2008, Tate *et al.* 2010, Purnama *et al.* 2014). To investigate the effects of NK cell activation during IAV infection, we cultured peripheral blood NK cells with IAV-infected autologous MDMs. MDMs were differentiated to a lung-like phenotype, modelling airway macrophage activity and infected as described previously (Cooper *et al.* 2016), resulting in a median of 29% of MDMs being positive for viral NP1 (Figure 9A). Following infection of the MDM monolayer, purified autologous NK cells were cultured with infected MDMs at an E:T ratio of 1:5 for 4-6h resulting in increased NK cell degranulation (P=0.031, Figure 9B). To assess NK cell cytotoxicity, MDM viability was measured by flow cytometry (Figure 9C and 9D). Co-culture with NK cells did not alter MDM viability when MDMs were uninfected (NT) or treated with UV-irradiated X31 (UV-X31) (P=0.2158 and P0.3848, Figure 9D). Although some variation in the uninfected NT NK culture was observed, this was not found to be significantly different to either the NT MDMs alone or the UV-X31 exposed co-culture (P=0.2158 and P=0.1250 respectively, Figure 9D). However, when MDMs were infected with live X31, MDM viability was reduced by 12% when NK cells were also present, relative to MDMs alone (P=0.0029, Figure 9D). MDM viability was also reduced relative to UV-X31 treated co-culture and uninfected co-culture (P=0.0420 and P=0.0186, Figure 9D) indicating that NK cells exerted a cytotoxic effect following live X31 infection.

3.6 NK cell contact with infected cells determines NK cell activation

Culture of purified autologous NK cells with IAV infected MDMs induced NK cell expression of antiviral molecules such as Granzyme-B and IFN-γ, as detected by flow cytometry (Figure 10 A and B and Supplementary Figure 2). Indeed, extracellular IFN-γ was only observed when NK cells were cultured with X31-infected MDMs (P=0.0078, Figure 10D). In addition, there was a non-significant trend towards increased extracellular Granzyme-B in X31-infected co-cultures (P=0.055, Figure 10E). $CD56^{bright}$ and $CD56^{dim}$ NK cells responded equivalently to culture with X31-infected MDMs, with all subsets producing IFN-γ (Figure 10C). These results suggest both cytokines and cytotoxic molecules are released by NK cells following contact with influenza infected cells.

Direct contact between NK cells and MDMs was essential for NK cell activation as separation of the two cells in a transwell system abrogated both Granzyme-B production and IFN-γ release (Figure 10). This suggests that changes to the MDM surface as a result of IAV infection may determine NK cell activation. HLA class I molecules play an important role in governing NK cell responses and are upregulated on IAV infected lung epithelial cells and macrophages (Figure 6 H and I and 11A). To investigate the effect of this change in surface HLA, HLA class I ligands on human MDMs were blocked with anti-HLA-A/B/C (clone W6/32) prior to culture with NK cells. Blocking with αHLA-ABC or isotype control did not affect NK cell activation in response to uninfected MDMs, suggesting that this antibody does not induce antibody-dependent cellular cytotoxicity. (Figure 11 B). However,

during culture with X31-infected MDMs, blocking class I HLA increased NK cell CD107a expression (P=0.031) indicating that HLA class I has inhibitory effects on NK cells during live influenza infection (Figure 11C). Despite this, NK cells still activate in response to influenza infected cells, suggesting the balance between NK cell activatory and inhibitory signalling is perturbed during contact with IAV-infected cells. These results suggest that NK cells are capable of a strong antiviral response following contact with influenza infected cells, with production and release of IFN-γ, Granzyme-B and significant cytotoxicity against infected macrophages.

4 Discussion

The role of NK cells in tissue specific responses is being increasingly recognized as they may represent an important early front-line defence during respiratory infection (Björkström *et al.* 2016, Peng and Tian 2017). In this study we have explored the NK cell response to influenza infection of human lung parenchyma and monocyte-derived macrophages. We identified early activation of NK cells in response to influenza infected cells, including IFN-γ and Granzyme-B production, degranulation and cytotoxicity. In addition, for the first time we demonstrate NK cell-mediated destruction of influenza-infected macrophages, indicating that NK cells may have an important role in regulating the effects of APCs during IAV infection (Nedvetzki *et al.* 2007, Bellora *et al.* 2010).

To explore the *ex vivo* function of human lung NK cells, NK cells were defined as CD45+CD3-CD56+ cells, a gating strategy designed to exclude ILC populations. Although a small population of ILC3s may be included in our analysis (50% of NCR- ILC3s express CD56) the total human lung ILC3 population comprise less than 0.025% of CD45+ cells and therefore would make a minimal contribution to our analysis (Spits *et al.* 2013, De Grove *et al.* 2016). However, consistent with previous reports, CD56+CD3- NK cells made up a significant proportion (18.55%) of CD45+ lymphocytes in the human lung and were found to be predominantly mature, canonical NK cells, corroborating the work of Marquardt *et al* 2017 (Michel *et al.* 2012, Wang *et al.* 2012, Marquardt *et al.* 2017).

Understanding the lung NK cell phenotype is important for understanding NK cell function during pulmonary health and disease. The differentiated and active NK cell phenotype described for NK cells both here and by Marquardt *et al* 2016 is interesting as unchecked cytotoxicity in this setting may have the capacity to impair lung function (Marquardt *et al.* 2017, Finch *et al.* 2018). Indeed NK cells taken from people with Chronic Obstructive Pulmonary Disease (COPD) were found to be more cytotoxic towards airway epithelia, a functional change which appeared intrinsic to the NK cell, indicating an altered activation state in this disease (Finch *et al.* 2018). NK cells isolated from the lungs have often been reported as hypofunctional following stimulation with PMA or K562 cell lines, a finding which might reflect important mechanisms of NK cell regulation in the pulmonary environment (Robinson *et al.* 1984, Michel *et al.* 2012, Wang *et al.* 2012, Marquardt *et al.* 2017). Yet in this study IAV infection of human lung explants was sufficient to activate NK cell degranulation. Both $CD56^{bright}$ and $CD56^{dim}$ NK cells were found to activate rapidly in response to IAV indicating that NK cells may aid early virus control within the lung.

As the lungs are a highly vascularized organ, it is possible the NK cells examined by this study may have been passing through the lungs during circulation (Marquardt *et al.* 2017). Indeed, the phenotype of lung-associated NK cells is more similar to the NK cells of the peripheral blood than other human

organs (Koopman *et al.* 2003, Marquardt *et al.* 2015, Lugthart *et al.* 2016, Montaldo *et al.* 2016). Although it is not possible to exclude the possibility that the phenotype reported in our study comes from the peripheral blood, the tissue was washed extensively and rested to remove contaminating blood cells prior to analysis. Analysis of the T cell phenotype in lung tissue utilizing this method supports this ability to remove blood lymphocytes, as only memory T cells are isolated from this organ with little to no presence of naïve T cells (Hutton *et al.* 2017). Moreover, we have identified a novel CD49a+CD69+CD103+ NK cell population from the human lung parenchyma not found in the blood. Interestingly, the lung possessed more CD49a+ NK cells compared to reports from the human liver (Marquardt *et al.* 2015).

To investigate the function of human lung CD49a+ NK cells we analyzed the CD107a expression of $CD56^{bright}$CD49a+ NK cells (Figure 7). We observed that a greater proportion of $CD56^{bright}$ CD49a+ NK cells activate in response to IAV infection compared to $CD56^{bright}$ CD49a- NK cells, an effect not seen with PMA/Ionomycin stimulation. This suggests that $CD56^{bright}$ CD49a+ NK cells may respond specifically to viral infection as the total potential of $CD56^{bright}$ CD49a+ NK cells is not dissimilar to $CD56^{bright}$ CD49a-. Lung CD49a+ NK cells may therefore represent a population of resident NK cells that can be induced to express a more robust recall response following prior exposure to common respiratory pathogens, such as IAV. Indeed, liver CD49a+ NK cells generated in influenza-infected mice were protective following adoptive transfer and subsequent influenza challenge, although murine lung CD49a+ NK cells were not protective in this model (Li *et al.* 2017). These experiments indicate that NK cell memory of influenza infection could exist within the adult human lung, although this requires further corroboration through analysis of transcription factor expression and epigenetic state. If so, the generation of such local mucosal immunity may have important implications for vaccine design, offering a possibility for increasing strain cross-reactivity and effectiveness (Peng and Tian 2017). However the full functional role of this $CD56^{bright}$CD49a+ population and the governing mechanisms remain to be elucidated.

As expected $CD56^{dim}$CD16-CD49a+ lung NK cells were not found to be more responsive to X31 infection, a finding that fits with the literature as only $CD56^{bright}$ populations have been associated with residency (Koopman *et al.* 2003, Marquardt *et al.* 2015, Lugthart *et al.* 2016, Montaldo *et al.* 2016). Some authors have suggested that $CD56^{dim}$CD16- NK cells represent contaminating CD3+CD56+ NKT cells (Zimmer *et al.* 2005, Grzywacz *et al.* 2007). However, as CD3+ cells were specifically excluded from our analysis (Figure 1) we consider it more likely that this population represent activated NK cells that have undergone CD56 and CD16 shedding (Penack *et al.* 2005, Grzywacz *et al.* 2007, Lutz *et al.* 2011, Romee *et al.* 2013). Therefore $CD56^{dim}$CD16-CD49a+ lung NK cells might represent functionally exhausted $CD56^{bright}$ CD49a+ cells. Interestingly, $CD56^{dim}$CD16- NK cells were also expanded in the peripheral blood of donors undergoing resection surgery when compared to healthy controls. A finding which may be due to demographic differences between the cohorts. Our preliminary data suggests that age did not affect the proportion of $CD56^{dim}$CD16- NK cells (Figure 2) however we cannot rule out an effect of disease and smoking status on the NK cell phenotype (Marquardt *et al.* 2017).

NK cell effector molecules IFN-γ and Gzm-B were produced by influenza-infected explants 24 hpi (Figure 8). The length of time taken in generating both IFN-γ and Granzyme-B by X31-infected tissue could suggest that this is a secondary response to initial inflammatory signaling through IFN-α and IFN-β, as there is some support for this in the literature (Hwang *et al.* 2012, Madera *et al.* 2016).

Interestingly extracellular Gzm-B appeared to wane by 6 hpi, only to rise again at 24 hpi in live-X31 infected tissue. However at the 2h timepoint extracellular Granzyme-B was greater in all conditions including uninfected (NT) tissue, this suggests that Granzyme-B release at this time-point may be a result of explant removal from the body or tissue preparation, as explants were washed prior to exposure to virus.

NK cell IFN-γ production and release was also measured from co-cultures with X31-infected MDMs and NK cells, an effect that was dependent on contact between the two cell types (Figure 10). Although CD56^{bright} NK cells have been suggested to dominate NK cell cytokine production, both CD56^{bright} and CD56^{dim} NK cells produced IFN-γ when MDMs were infected with live X31, suggesting that there may be a common mechanism of activation between the two subtypes toward influenza (Cooper *et al.* 2001, Ferlazzo *et al.* 2004). This could include the NKp46 or NKG2D activating receptors as well as activating or inhibitory KIR (Mandelboim *et al.* 2001, Draghi *et al.* 2007, Achdout *et al.* 2008). However, these molecules are differentially expressed by CD56^{bright} and CD56^{dim} NK cells and it is possible that NK cell subsets are activated by different mechanisms during influenza infection (Jacobs *et al.* 2001, Poli *et al.* 2009). Interestingly, Granzyme-B release appeared less dependent on contact between NK cells and infected MDMs, however as Granzyme-B is released within the immune synapse this could limit detection of changes in the amount of this molecule. Although the differences between cells treated with UV-X31 and live X31 have not been thoroughly explored here, no NK cell response was observed towards UV-infected macrophages, either in the tissue explant or MDM infection. This suggests that NK cells are responding to changes on the target cell, in response to the intracellular replication of live influenza.

The upregulation of HLA class I molecules during IAV infection appeared to be inhibitory to NK cells, as blocking HLA class I increased NK cell degranulation. This might represent viral evasion of the NK cell response (Mahmoud *et al.* 2016). Alternatively, HLA class I upregulation could also reflect a host strategy for increased antigen presentation to CD8+ T cells. An inhibitory role of the HLA class I suggests that NK cell activation to IAV-infected cells may depend on upregulation of concomitant ligands for activating receptors, such as NKp46 and NKG2D on the target cell surface (Mandelboim *et al.* 2001, Draghi *et al.* 2007, Achdout *et al.* 2008). Interestingly, cigarette smoke has been shown to prime the NK cell response to viral infection through increased expression of NKG2D ligands in a murine model of COPD (Motz *et al.* 2010). Unfortunately, due to flow cytometry channel limits it was not possible to investigate tissue ligand expression in the experiments presented here.

Cancer resection is one of the few available sources of human lung tissue, but disease state, smoking history and medication remain confounding factors in the use of this material (Marquardt *et al.* 2017). Furthermore, the heterogeneity between individuals is reflected in the range of NK cell functional responses and marker expression. Despite these caveats, the NK cell phenotype from the human lung is consistent with healthy mice in terms of maturity and differentiation, and functional results were further confirmed in a co-culture model of IAV infection. (Michel *et al.* 2012, Wang *et al.* 2012). Analysis of human lung-resident NK cell populations would not be possible without human lung tissue and *ex vivo* infection enables the characterization of NK cell function in a relevant context of human disease.

In conclusion, we identify a unique and putative resident CD56^{bright} CD49a+ lung NK cell population which underwent greater levels of activation during IAV infection. We speculate that CD49a+ NK cells could represent a lung resident population of NK cells trained by the respiratory environment. Further exploration of this NK cell phenotype is required to understand whether such local mucosal immunity could be manipulated to broaden IAV vaccine cross-reactivity and efficacy. As NK cells make up around a quarter of parenchymal lymphocytes and respond rapidly to IAV infection, NK cells may be well placed to provide early and broad innate immunity to IAV infection in humans.

5 Author contributions

Data acquisition, analysis and interpretation was provided by GC, KO and KS. All authors contributed to the drafting of manuscript for important intellectual content and manuscript conception and design.

6 References

Abdul-Careem, M. F., M. F. Mian, G. Yue, A. Gillgrass, M. J. Chenoweth, N. G. Barra, M. V. Chew, T. Chan, A. A. Al-Garawi, M. Jordana and A. A. Ashkar (2012). "Critical role of natural killer cells in lung immunopathology during influenza infection in mice." J Infect Dis **206**(2): 167-177.

Achdout, H., I. Manaster and O. Mandelboim (2008). "Influenza virus infection augments NK cell inhibition through reorganization of major histocompatibility complex class I proteins." J Virol **82**(16): 8030-8037.

Bellora, F., R. Castriconi, A. Dondero, G. Reggiardo, L. Moretta, A. Mantovani, A. Moretta and C. Bottino (2010). "The interaction of human natural killer cells with either unpolarized or polarized macrophages results in different functional outcomes." Proc Natl Acad Sci U S A **107**(50): 21659-21664.

Björkström, N. K., H.-G. Ljunggren and J. Michaëlsson (2016). "Emerging insights into natural killer cells in human peripheral tissues." Nature Reviews Immunology **16**: 310 - 320.

Bjorkstrom, N. K., P. Riese, F. Heuts, S. Andersson, C. Fauriat, M. A. Ivarsson, A. T. Bjorklund, M. Flodstrom-Tullberg, J. Michaelsson, M. E. Rottenberg, C. A. Guzman, H. G. Ljunggren and K. J. Malmberg (2010). "Expression patterns of NKG2A, KIR, and CD57 define a process of CD56dim NK-cell differentiation uncoupled from NK-cell education." Blood **116**(19): 3853-3864.

Cooper, G. E., Z. C. Pounce, J. C. Wallington, L. Y. Bastidas-Legarda, B. Nicholas, C. Chidomere, E. C. Robinson, K. Martin, A. S. Tocheva, M. Christodoulides, R. Djukanovic, T. M. A. Wilkinson and K. J. Staples (2016). "Viral Inhibition of Bacterial Phagocytosis by Human Macrophages: Redundant Role of CD36." PLOS ONE **11**(10): e0163889.

Cooper, M. A., T. A. Fehniger, S. C. Turner, K. S. Chen, B. A. Ghaheri, T. Ghayur, W. E. Carson and M. A. Caligiuri (2001). "Human natural killer cells: a unique innate immunoregulatory role for the CD56(bright) subset." Blood **97**(10): 3146-3151.

De Grove, K. C., S. Provoost, F. M. Verhamme, K. R. Bracke, G. F. Joos, T. Maes and G. G. Brusselle (2016). "Characterization and Quantification of Innate Lymphoid Cell Subsets in Human Lung." PLoS One **11**(1): e0145961.

De Maria, A., F. Bozzano, C. Cantoni and L. Moretta (2011). "Revisiting human natural killer cell subset function revealed cytolytic CD56(dim)CD16+ NK cells as rapid producers of abundant IFN-gamma on activation." Proc Natl Acad Sci U S A **108**(2): 728-732.

Dou, Y., B. Fu, R. Sun, W. Li, W. Hu, Z. Tian and H. Wei (2015). "Influenza vaccine induces intracellular immune memory of human NK cells." PLoS One **10**(3): e0121258.

Draghi, M., A. Pashine, B. Sanjanwala, K. Gendzekhadze, C. Cantoni, D. Cosman, A. Moretta, N. M. Valiante and P. Parham (2007). "NKp46 and NKG2D recognition of infected dendritic cells is necessary for NK cell activation in the human response to influenza infection." J Immunol **178**(5): 2688-2698.

Ferlazzo, G., D. Thomas, S. L. Lin, K. Goodman, B. Morandi, W. A. Muller, A. Moretta and C. Munz (2004). "The abundant NK cells in human secondary lymphoid tissues require activation to express killer cell Ig-like receptors and become cytolytic." J Immunol **172**(3): 1455-1462.

Finch, D. K., V. R. Stolberg, J. Ferguson, H. Alikaj, M. R. Kady, B. W. Richmond, V. V. Polosukhin, T. S. Blackwell, L. McCloskey, J. L. Curtis and C. M. Freeman (2018). "Lung Dendritic Cells Drive NK Cytotoxicity in Chronic Obstructive Pulmonary Disease via IL-15Ralpha." Am J Respir Crit Care Med: In press.

Freeman, C. M., V. R. Stolberg, S. Crudgington, F. J. Martinez, M. K. Han, S. W. Chensue, D. A. Arenberg, C. A. Meldrum, L. McCloskey and J. L. Curtis (2014). "Human CD56+ cytotoxic lung lymphocytes kill autologous lung cells in chronic obstructive pulmonary disease." PLoS One **9**(7): e103840.

Freud, A. G., A. Yokohama, B. Becknell, M. T. Lee, H. C. Mao, A. K. Ferketich and M. A. Caligiuri (2006). "Evidence for discrete stages of human natural killer cell differentiation in vivo." J Exp Med **203**(4): 1033-1043.

Gazit, R., R. Gruda, M. Elboim, T. I. Arnon, G. Katz, H. Achdout, J. Hanna, U. Qimron, G. Landau, E. Greenbaum, Z. Zakay-Rones, A. Porgador and O. Mandelboim (2006). "Lethal influenza infection in the absence of the natural killer cell receptor gene Ncr1." Nat Immunol **7**(5): 517-523.

Greenberg, H. B. and P. A. Piedra (2004). "Immunization against viral respiratory disease: a review." Pediatr Infect Dis J **23**(11 Suppl): S254-261.

Grzywacz, B., N. Kataria and M. R. Verneris (2007). "CD56dimCD16+ NK cells downregulate CD16 following target cell induced activation of matrix metalloproteinases." Leukemia **21**(2): 356-359.

Guma, M., M. Budt, A. Saez, T. Brckalo, H. Hengel, A. Angulo and M. Lopez-Botet (2006). "Expansion of CD94/NKG2C+ NK cells in response to human cytomegalovirus-infected fibroblasts." Blood **107**(9): 3624-3631.

He, X. S., M. Draghi, K. Mahmood, T. H. Holmes, G. W. Kemble, C. L. Dekker, A. M. Arvin, P. Parham and H. B. Greenberg (2004). "T cell-dependent production of IFN-gamma by NK cells in response to influenza A virus." J Clin Invest **114**(12): 1812-1819.

He, X. S., T. H. Holmes, C. Zhang, K. Mahmood, G. W. Kemble, D. B. Lewis, C. L. Dekker, H. B. Greenberg and A. M. Arvin (2006). "Cellular immune responses in children and adults receiving inactivated or live attenuated influenza vaccines." J Virol **80**(23): 11756-11766.

Hutton, A. J., M. E. Polak, C. M. Spalluto, J. C. Wallington, C. Pickard, K. J. Staples, J. A. Warner and T. M. A. Wilkinson (2017). "Human Lung Fibroblasts Present Bacterial Antigens to Autologous Lung Th Cells." The Journal of Immunology **198**(1): 110-118.

564 Hwang, I., J. M. Scott, T. Kakarla, D. M. Duriancik, S. Choi, C. Cho, T. Lee, H. Park, A. R. French,
565 E. Beli, E. Gardner and S. Kim (2012). "Activation mechanisms of natural killer cells during influenza
566 virus infection." PLoS One **7**(12): e51858.

567 Jacobs, R., G. Hintzen, A. Kemper, K. Beul, S. Kempf, G. Behrens, K. W. Sykora and R. E. Schmidt
568 (2001). "CD56bright cells differ in their KIR repertoire and cytotoxic features from CD56dim NK
569 cells." Eur J Immunol **31**(10): 3121-3127.

570 Jost, S., H. Quillay, J. Reardon, E. Peterson, R. P. Simmons, B. A. Parry, N. N. Bryant, W. D. Binder
571 and M. Altfeld (2011). "Changes in cytokine levels and NK cell activation associated with influenza."
572 PLoS One **6**(9): e25060.

573 Kim, H. M., Y.-W. Lee, K.-J. Lee, H. S. Kim, S. W. Cho, N. van Rooijen, Y. Guan and S. H. Seo
574 (2008). "Alveolar Macrophages Are Indispensable for Controlling Influenza Viruses in Lungs of Pigs."
575 Journal of Virology **82**(9): 4265-4274.

576 Koopman, L. A., H. D. Kopcow, B. Rybalov, J. E. Boyson, J. S. Orange, F. Schatz, R. Masch, C. J.
577 Lockwood, A. D. Schachter, P. J. Park and J. L. Strominger (2003). "Human Decidual Natural Killer
578 Cells Are a Unique NK Cell Subset with Immunomodulatory Potential." The Journal of Experimental
579 Medicine **198**(8): 1201-1212.

580 Krammer, F. and P. Palese (2015). "Advances in the development of influenza virus vaccines." Nat
581 Rev Drug Discov **14**(3): 167-182.

582 Kumar, P., M. S. Thakar, W. Ouyang and S. Malarkannan (2013). "IL-22 from conventional NK cells
583 is epithelial regenerative and inflammation protective during influenza infection." Mucosal Immunol
584 **6**(1): 69-82.

585 Li, T., J. Wang, Y. Wang, Y. Chen, H. Wei, R. Sun and Z. Tian (2017). "Respiratory Influenza Virus
586 Infection Induces Memory-like Liver NK Cells in Mice." J Immunol **198**(3): 1242-1252.

587 Long, B. R., J. Michaelsson, C. P. Loo, W. M. Ballan, B. A. Vu, F. M. Hecht, L. L. Lanier, J. M.
588 Chapman and D. F. Nixon (2008). "Elevated frequency of gamma interferon-producing NK cells in
589 healthy adults vaccinated against influenza virus." Clin Vaccine Immunol **15**(1): 120-130.

590 Lopez-Verges, S., J. M. Milush, S. Pandey, V. A. York, J. Arakawa-Hoyt, H. Pircher, P. J. Norris, D.
591 F. Nixon and L. L. Lanier (2010). "CD57 defines a functionally distinct population of mature NK cells
592 in the human CD56dimCD16+ NK-cell subset." Blood **116**(19): 3865-3874.

593 Lugthart, G., J. E. Melsen, C. Vervat, M. M. van Ostaijen-ten Dam, W. E. Corver, D. L. Roelen, J. van
594 Bergen, M. J. D. van Tol, A. C. Lankester and M. W. Schilham (2016). "Human Lymphoid Tissues
595 Harbor a Distinct CD69+CXCR6+ NK Cell Population." The Journal of Immunology **197**(1): 78-84.

596 Lutz, C. T., A. Karapetyan, A. Al-Attar, B. J. Shelton, K. J. Holt, J. H. Tucker and S. R. Presnell (2011).
597 "Human NK Cells Proliferate and Die In Vivo More Rapidly than T Cells in Healthy Young and
598 Elderly Adults." The Journal of Immunology **186**(8): 4590-4598.

599 Madera, S., M. Rapp, M. A. Firth, J. N. Beilke, L. L. Lanier and J. C. Sun (2016). "Type I IFN promotes
600 NK cell expansion during viral infection by protecting NK cells against fratricide." J Exp Med **213**(2):
601 225-233.

602 Mahmoud, A. B., M. M. Tu, A. Wight, H. S. Zein, M. M. Rahim, S. H. Lee, H. S. Sekhon, E. G. Brown
603 and A. P. Makrigiannis (2016). "Influenza Virus Targets Class I MHC-Educated NK Cells for
604 Immunoevasion." PLoS Pathog **12**(2): e1005446.

Mandelboim, O., N. Lieberman, M. Lev, L. Paul, T. I. Arnon, Y. Bushkin, D. M. Davis, J. L. Strominger, J. W. Yewdell and A. Porgador (2001). "Recognition of haemagglutinins on virus-infected cells by NKp46 activates lysis by human NK cells." Nature **409**(6823): 1055-1060.

Marquardt, N., V. Beziat, S. Nystrom, J. Hengst, M. A. Ivarsson, E. Kekalainen, H. Johansson, J. Mjosberg, M. Westgren, T. O. Lankisch, H. Wedemeyer, E. C. Ellis, H. G. Ljunggren, J. Michaelsson and N. K. Bjorkstrom (2015). "Cutting edge: identification and characterization of human intrahepatic CD49a+ NK cells." J Immunol **194**(6): 2467-2471.

Marquardt, N., E. Kekäläinen, P. Chen, E. Kvedaraite, J. N. Wilson, M. A. Ivarsson, J. Mjösberg, L. Berglin, J. Säfholm, M. L. Manson, M. Adner, M. Al-Ameri, P. Bergman, A.-C. Orre, M. Svensson, B. Dahlén, S.-E. Dahlén, H.-G. Ljunggren and J. Michaëlsson (2017). "Human lung natural killer cells are predominantly comprised of highly differentiated hypofunctional CD69-CD56dim cells." Journal of Allergy and Clinical Immunology **139**(4): 1321-1330.

McKendry, R. T., C. M. Spalluto, H. Burke, B. Nicholas, D. Cellura, A. Al-Shamkhani, K. J. Staples and T. M. A. Wilkinson (2016). "Dysregulation of Antiviral Function of CD8(+) T Cells in the Chronic Obstructive Pulmonary Disease Lung. Role of the PD-1–PD-L1 Axis." American Journal of Respiratory and Critical Care Medicine **193**(6): 642-651.

Michel, T., A. Poli, O. Domingues, M. Mauffray, M. Theresine, N. H. Brons, F. Hentges and J. Zimmer (2012). "Mouse lung and spleen natural killer cells have phenotypic and functional differences, in part influenced by macrophages." PLoS One **7**(12): e51230.

Middleton, D. and F. Gonzelez (2010). "The extensive polymorphism of KIR genes." Immunology **129**(1): 8-19.

Montaldo, E., P. Vacca, L. Chiossone, D. Croxatto, F. Loiacono, S. Martini, S. Ferrero, T. Walzer, L. Moretta and M. C. Mingari (2016). "Unique Eomes(+) NK Cell Subsets Are Present in Uterus and Decidua During Early Pregnancy." Front Immunol **6**: 646.

Moretta, L. (2010). "Dissecting CD56dim human NK cells." Blood **116**(19): 3689-3691.

Mossad, S. B. (2016). "Influenza: Still more important than Zika virus in 2016-2017." Cleve Clin J Med **83**(11): 836-840.

Motz, G. T., B. L. Eppert, B. W. Wortham, R. M. Amos-Kroohs, J. L. Flury, S. C. Wesselkamper and M. T. Borchers (2010). "Chronic Cigarette Smoke Exposure Primes NK Cell Activation in a Mouse Model of Chronic Obstructive Pulmonary Disease." The Journal of Immunology **184**(8): 4460-4469.

Nagler, A., L. L. Lanier, S. Cwirla and J. H. Phillips (1989). "Comparative studies of human FcRIII-positive and negative natural killer cells." J Immunol **143**(10): 3183-3191.

Nedvetzki, S., S. Sowinski, R. A. Eagle, J. Harris, F. Vely, D. Pende, J. Trowsdale, E. Vivier, S. Gordon and D. M. Davis (2007). "Reciprocal regulation of human natural killer cells and macrophages associated with distinct immune synapses." Blood **109**(9): 3776-3785.

Nicholas, B., K. J. Staples, S. Moese, E. Meldrum, J. Ward, P. Dennison, T. Havelock, T. S. C. Hinks, K. Amer, E. Woo, M. Chamberlain, N. Singh, M. North, S. Pink, T. M. A. Wilkinson and R. Djukanović (2015). "A novel lung explant model for the ex vivo study of efficacy and mechanisms of anti-influenza drugs." Journal of immunology (Baltimore, Md. : 1950) **194**(12): 6144-6154.

Nogusa, S., B. W. Ritz, S. H. Kassim, S. R. Jennings and E. M. Gardner (2008). "Characterization of age-related changes in natural killer cells during primary influenza infection in mice." Mech Ageing Dev **129**(4): 223-230.

Penack, O., C. Gentilini, L. Fischer, A. M. Asemissen, C. Scheibenbogen, E. Thiel and L. Uharek (2005). "CD56dimCD16neg cells are responsible for natural cytotoxicity against tumor targets." Leukemia **19**(5): 835-840.

Peng, H. and Z. Tian (2017). "Natural Killer Cell Memory: Progress and Implications." Front Immunol **8**: 1143.

Poli, A., T. Michel, M. Theresine, E. Andres, F. Hentges and J. Zimmer (2009). "CD56bright natural killer (NK) cells: an important NK cell subset." Immunology **126**(4): 458-465.

Purnama, C., S. L. Ng, P. Tetlak, Y. A. Setiagani, M. Kandasamy, S. Baalasubramanian, K. Karjalainen and C. Ruedl (2014). "Transient ablation of alveolar macrophages leads to massive pathology of influenza infection without affecting cellular adaptive immunity." Eur J Immunol **44**(7): 2003-2012.

Robinson, B. W., P. Pinkston and R. G. Crystal (1984). "Natural killer cells are present in the normal human lung but are functionally impotent." J Clin Invest **74**(3): 942-950.

Romagnani, C., K. Juelke, M. Falco, B. Morandi, A. D'Agostino, R. Costa, G. Ratto, G. Forte, P. Carrega, G. Lui, R. Conte, T. Strowig, A. Moretta, C. Munz, A. Thiel, L. Moretta and G. Ferlazzo (2007). "CD56brightCD16- killer Ig-like receptor- NK cells display longer telomeres and acquire features of CD56dim NK cells upon activation." J Immunol **178**(8): 4947-4955.

Romee, R., B. Foley, T. Lenvik, Y. Wang, B. Zhang, D. Ankarlo, X. Luo, S. Cooley, M. Verneris, B. Walcheck and J. Miller (2013). "NK cell CD16 surface expression and function is regulated by a disintegrin and metalloprotease-17 (ADAM17)." Blood **121**(18): 3599-3608.

Schlums, H., F. Cichocki, B. Tesi, J. Theorell, V. Beziat, T. D. Holmes, H. Han, S. C. Chiang, B. Foley, K. Mattsson, S. Larsson, M. Schaffer, K. J. Malmberg, H. G. Ljunggren, J. S. Miller and Y. T. Bryceson (2015). "Cytomegalovirus infection drives adaptive epigenetic diversification of NK cells with altered signaling and effector function." Immunity **42**(3): 443-456.

Spits, H., D. Artis, M. Colonna, A. Diefenbach, J. P. Di Santo, G. Eberl, S. Koyasu, R. M. Locksley, A. N. McKenzie, R. E. Mebius, F. Powrie and E. Vivier (2013). "Innate lymphoid cells--a proposal for uniform nomenclature." Nat Rev Immunol **13**(2): 145-149.

Staples, K. J., T. S. C. Hinks, J. A. Ward, V. Gunn, C. Smith and R. Djukanović (2012). "Phenotypic characterization of lung macrophages in asthmatic patients: Overexpression of CCL17." Journal of Allergy and Clinical Immunology **130**(6): 1404-1412.e1407.

Staples, K. J., B. Nicholas, R. T. McKendry, C. M. Spalluto, J. C. Wallington, C. W. Bragg, E. C. Robinson, K. Martin, R. Djukanovic and T. M. Wilkinson (2015). "Viral infection of human lung macrophages increases PDL1 expression via IFNbeta." PLoS One **10**(3): e0121527.

Stein-Streilein, J. and J. Guffee (1986). "In vivo treatment of mice and hamsters with antibodies to asialo GM1 increases morbidity and mortality to pulmonary influenza infection." The Journal of Immunology **136**(4): 1435-1441.

Stohr, K. (2002). "Influenza--WHO cares." Lancet Infect Dis **2**(9): 517.

Tate, M. D., D. L. Pickett, N. van Rooijen, A. G. Brooks and P. C. Reading (2010). "Critical role of airway macrophages in modulating disease severity during influenza virus infection of mice." J Virol **84**(15): 7569-7580.

Taubenberger, J. K. and J. C. Kash (2010). "Influenza Virus Evolution, Host Adaptation, and Pandemic Formation." Cell Host & Microbe **7**(6): 440-451.

688 Uhrberg, M., P. Parham and P. Wernet (2002). "Definition of gene content for nine common group B
689 haplotypes of the Caucasoid population: KIR haplotypes contain between seven and eleven KIR
690 genes." Immunogenetics **54**(4): 221-229.

691 Vivier, E., J. A. Nunes and F. Vely (2004). "Natural killer cell signaling pathways." Science **306**(5701):
692 1517-1519.

693 Vivier, E., E. Tomasello, M. Baratin, T. Walzer and S. Ugolini (2008). "Functions of natural killer
694 cells." Nat Immunol **9**(5): 503-510.

695 Wang, J., F. Li, M. Zheng, R. Sun, H. Wei and Z. Tian (2012). "Lung natural killer cells in mice:
696 phenotype and response to respiratory infection." Immunology **137**(1): 37-47.

697 Wong, M. T., D. E. Ong, F. S. Lim, K. W. Teng, N. McGovern, S. Narayanan, W. Q. Ho, D. Cerny,
698 H. K. Tan, R. Anicete, B. K. Tan, T. K. Lim, C. Y. Chan, P. C. Cheow, S. Y. Lee, A. Takano, E. H.
699 Tan, J. K. Tam, E. Y. Tan, J. K. Chan, K. Fink, A. Bertoletti, F. Ginhoux, M. A. Curotto de Lafaille
700 and E. W. Newell (2016). "A High-Dimensional Atlas of Human T Cell Diversity Reveals Tissue-
701 Specific Trafficking and Cytokine Signatures." Immunity **45**(2): 442-456.

702 Yoon, J. C., C. M. Yang, Y. Song and J. M. Lee (2016). "Natural killer cells in hepatitis C: Current
703 progress." World Journal of Gastroenterology **22**(4): 1449-1460.

704 Zhou, G., S. W. Juang and K. P. Kane (2013). "NK cells exacerbate the pathology of influenza virus
705 infection in mice." Eur J Immunol **43**(4): 929-938.

706 Zhou, K., J. Wang, A. Li, W. Zhao, D. Wang, W. Zhang, J. Yan, G. F. Gao, W. Liu and M. Fang
707 (2016). "Swift and Strong NK Cell Responses Protect 129 Mice against High-Dose Influenza Virus
708 Infection." J Immunol **196**(4): 1842-1854.

709 Zimmer, J., E. Andres and F. Hentges (2005). "NK cell subsets and CD107a mobilization assay."
710 Leukemia **19**(10): 1849-1851; author reply 1857.

711 ## 7 Figure legends

712 **Figure 1:** Lung-associated NK cells are highly differentiated and similar to the peripheral blood of
713 healthy donors (H-PB) and those undergoing cancer resection (CR-PB). (**A,**) Representative gating
714 strategy to define NK cells and NK cell subpopulations isolated from human lung parenchyma. (**B**)
715 Quantification of lung CD45+ lymphocytes, N=23. (**C, D, E**) Proportions of $CD56^{bright}$,
716 $CD56^{dim}$CD16+ and $CD56^{dim}$CD16- NK cells in healthy peripheral blood (H-PB, N=14), lung tissue
717 (N=23) and matched blood (CR-PB, N=23).

718 **Figure 2:** NK cell subpopulation proportions are not affected by age. $CD56^{bright}$, $CD56^{dim}$CD16+ and
719 $CD56^{dim}$CD16- proportions in peripheral blood of healthy donors aged 22-40 (N=10) and 56-72
720 (N=12). Statistical analysis by Mann Whitney U test, lines describe medians.

721 **Figure 3:** CD57, CD158b and NKG2C expression on lung and blood NK cells. CD57 (**A**) and CD158b
722 (**C**) expression on NK cell subsets in peripheral blood of healthy controls (H-PB N=11) and peripheral
723 blood (CR-PB) and lung of cancer resection patients (N=9). Lines describe medians, comparison
724 between healthy and resection blood by Mann-Whitney U test and between lung and CR-PB by
725 Wilcoxon signed-rank test. (**B,D**) CD57 and CD158b expression on $CD56^{bright}$, $CD56^{dim}$CD16+ and
726 $CD56^{dim}$CD16- NK cells from the blood and lung. Statistical analysis of H-PB to CR-PB by Kruskal-
727 Wallis test with Dunn's multiple comparison correction and CR-PB to lung tissue by Friedman's test
728 with Dunn's multiple comparison correction. (**E**) Representative flow cytometry plot describing lung
729 NK cell CD57 and CD158b expression. (**F**) CD57 and CD158b expression on NK cells from the lung

and matched blood (CR-PB (N=7). Statistical analysis by Friedman's test with Dunn's multiple comparison correction. (**G**) NKG2C expression on healthy controls (N=5), cancer resection donor blood and lung tissue (N=19). (**H**) NKG2C expression on $CD56^{bright}$, $CD56^{dim}CD16+$ and $CD56^{dim}CD16-$ NK cells from the blood and lung.

Figure 4: Distinct NK cell populations are present in the blood, but not the lung. (**A,C,E**) Flow cytometric analysis of CD49a (N=22), CD103 (N=8) and CD69 (N=8) expression on lung and blood NK cells. Statistical analysis performed by Wilcoxon signed-rank test. Lines describe medians. (**B,D,F**) Residency marker expression on $CD56^{bright}$ and $CD56^{dim}$ NK cell subsets. Statistical analysis by Friedman's test with Dunn's multiple comparison correction.

Figure 5: $CD56^{bright}$ CD49a+ lung NK cells co-express CD69 and CD103. (**A**) Gating strategy to define co-expression of CD69 and CD103 on CD49a+ and CD49a- populations of $CD56^{bright}$ NK cells isolated from the lung (**A**) and blood (CR-PB) (**B**). (**C**) t-SNE plot of $CD56^{bright}$ NK cells in matched blood (blue) and lung (orange) based on CD49a, CD69 and CD103 expression (N=16, 8 individuals). From each sample 300 events were randomly selected. Perplexity=20, 1000 iterations. (**D**) t-SNE plot of CD56bright NK cells isolated from the lungs based on CD49a, CD69 and CD103 expression (N=8). Cells are coloured according to expression of each marker, showing single-positive (SP), double-positive (DP) and triple-positive (TP) populations. From each sample 600 events were randomly selected. Perplexity=20, 1000 Iterations. (**E**) Quantification of CD69 and CD103 expression of CD49a+ and CD49a- $CD56^{bright}$ NK cell populations of the lung and blood. Lines described medians, statistical analysis by Friedman's test with Dun's correction (N=8). Overall P value <0.001 (**F, G**) Quantification of residency marker expression on $CD56^{bright}$ NK cells of matched blood (**F**) and lung (**G**). Key as shown in Figure 5D.

Figure 6: Influenza X31 infection in human lung explants (**A**) Representative flow cytometry plot defining lung epithelia as CD45-EpCAM+ cells. (**B, C**) Influenza Nucleoprotein1 (NP1) expression in X31 infected epithelia. (**D**) Representative flow cytometry plot defining lung macrophages as CD45+HLA-DR+ cells. (**E,F**) Influenza NP1 expression in X31 infected macrophages. (G,**H**) Expression of HLA-A/B/C on epithelial cells (**G**) and macrophages (**H**) with and without X31 infection, as defined by NP1 expression. Lines describe medians, statistical analyses performed by Wilcoxon-signed rank test (N=7).

Figure 7: NK cell activation in X31-infected human lung explants. (**A**,**B**) Representative flow plot and quantification of surface CD107a on explant NK cells 24 hpi (N=6). (**C**) Surface CD107a on NK cell subsets 24h after X31 infection (N=5). Uninfected (NT) background CD107a expression was subtracted. (**D,E**) CD49a+ and C49a- NK cell degranulation of $CD56^{bright}$ (**D**) and $CD56^{dim}CD16-$ (**E**) NK cells following X31 infection and PMA/I stimulation of lung explants (N=6). (**F,G**) Extracellular Granzyme-B and IFN-γ in explant supernatants 24h post infection with X31 (N=8). Lines describe medians, statistical analysis performed by Wilcoxon-signed rank test.

Figure 8: Explant response to X31 infection over time (**A**) NK cell surface expression of CD107a (**B,C**) Extracellular secretion of IFN-γ (**B**) and Granzyme-B (**C**) from infected lung tissue (N=3, except 6h N=2). Lines describe mean and SEM.

Figure 9: Peripheral blood NK cells are cytotoxic towards X31-infected cells. (**A**) X31 infection of monocyte-derived macrophages (MDMs) was determined by flow cytometric analysis of NP1 expression (N=6). (**B**) Uninfected (NT), UV-irradiated X31 and live X31 infected MDMs were cultured with autologous peripheral blood NK cells for 4-6h. NK cell degranulation was determined

by flow cytometric analysis of surface CD107a (N=5). (**C, D**) Following culture with NK cells, MDM viability was measured by uptake of amine-binding dye and analysed by flow cytometry (N=10). Representative gating for MDM viability. Fixable dead stain, viability gating defined through heat killed control. (**C**) Representative gating of X31-infected MDM viability. Lines describe medians, statistical analysis by Wilcoxon signed-rank test.

Figure 10: Peripheral blood NK cells produce IFN-γ and Granzyme-B after contact with X31-infected cells. (**A,B**) Intracellular accumulation of Granzyme-B and IFN-γ was measured by flow cytometry 6h after culture with X31-infected MDMs. Physical separation of MDMs and NK cells in a transwell system abrogated IFN-γ and Granzyme-B production (N=6). (**C**) Intracellular IFN-γ of $CD56^{bright}$ and $CD56^{dim}$ NK cell subsets when cultured with MDMs treated with UV-irradiated X31 and live-X31. (**D,E**) Extracellular secretion of Granzyme-B (**D**) and IFN-γ (**E**). Lines describe medians, statistical analysis by Wilcoxon signed-rank test.

Figure 11: Blocking class I HLA increases NK cell degranulation during culture with X31-infected macrophages. (**A**) MDM HLA-A/B/C expression 24h after uninfected (NT) UV-irradiated and live X31 infection (N=5). (**B**) Background NK cell degranulation following culture with uninfected macrophages when macrophages were treated with αHLA or isotype control for 20min prior to addition of NK cells (IgG2a) (N=5). (**C**) 24h post-infection MDMs were incubated with antibody against HLA-A/B/C for 20min prior to co-culture with NK cells. NK cell degranulation was measured by flow cytometry (N=5). Lines describe medians. Statistical analyses performed by Wilcoxon-signed rank test.

8 Tables

Table 1: Cohort demographics for resection donors and healthy controls. Median values and italicised interquartile range are shown. NA = Data not available. * indicates additional locations of resection surgeries. [1] Two-tailed Mann Whitney Test [2] Fisher's Test [3] Chi-square Test

	Cancer resection donors	Healthy control donors (phenotyping)	P-value
Number of patients	35	15	
Age (yr)	70 *(9.75)*	24 *(8)*	<0.0001[1]
M/F	21/14	10/5	0.7570 [2]
Smoking status, never/ex/current/unknown	5/22/7/1	10/4/1	0.0013 [3]
Pack-years of smoking	40 *(33.75)*	NA	NA
FEV1%	86 *(28.5)*	NA	NA
FEV1/FVC ratio	0.65 *(0.15)*	NA	NA
Resection Location, LUL/LLL/RUL/ RML/RLL	8/7/11/3/3 *1 RUL+LUL *1 RUL+RML *1 Left pneumonectomy	NA	NA

Table 2: Cohort demographics for age comparison study. Median values and italicised interquartile range are shown. [1]Two-tailed Mann-Whitney [2] Fisher's test [3]Chi-squared test.

	Healthy control (Under 40)	Healthy control (Over 40)	P-value
Number of patients	10	12	
Age (yr)	34 *(5.5)*	66.5 *(7)*	<0.0001[1]
M/F	4/6	4/8	0.5315[2]
Smoking status, never/ex/current	6/3/1	6/6/0	0.3998[3]
Pack-years of smoking	0 *(1.605)*	2 *(20)*	0.2332[1]
FEV1%	97 *(17.75)*	108 *(16.5)*	0.0143[1]
FEV1/FVC ratio	0.84 *(8.5)*	0.78 *(2.75)*	0.1945[1]

9 Conflict of Interest

KS and TW have applied for a patent for the explant infection model (PCT/GB2010/050821 "Ex Vivo Modelling of Therapeutic Interventions"). They report funding from GSK Biologicals SA and

AstraZeneca outside of the submitted work. GC, KO and SK have no potential conflict of interest to declare.

10 Funding

This work was part funded by the BMA HC Roscoe Award 2013 to KS and TW. GC was funded by a 4 year MRC PhD studentship. The authors also gratefully acknowledge the support of the Southampton AAIR charity.

11 Acknowledgments

The authors wish to thank Richard Jewell and Dr Carolann MacGuire of the University of Southampton, Faculty of Medicine, Flow Cytometry Unit. We would also like to express our appreciation to Benjamin Johnson, Carine Fixmer and the rest of the Target Lung staff who co-ordinated lung tissue samples. We extend our gratitude to all the volunteers who provided lung and blood samples.

12 Abbreviations

APC: Antigen presenting cell

COPD: Chronic obstructive pulmonary disease

CR-PB: Peripheral blood from cancer resection donor

E: T: Effector: target

GzmB: Granzyme-B

H-PB: Healthy peripheral blood

IAV: Influenza A virus

ILC: Innate Lymphoid Cell

IQR: Interquartile Range

MACS: Magnetic-activated cell sorting

MDM: Monocyte-derived macrophage

MOI: Multiplicity of infection

NCR: Natural Cytotoxicity Receptor

NTHi: Non-typeable *Haemophilus influenzae*

NP1: Nucleoprotein 1

PBMC: Peripheral blood mononuclear cells

PMA/I: Phorbol myristate acetate/Ionomycin

SMFI: Specific mean fluorescence intensity

ssRNA: Single-stranded ribonucleic acid

TCR: T cell receptor

Figure 1.TIF

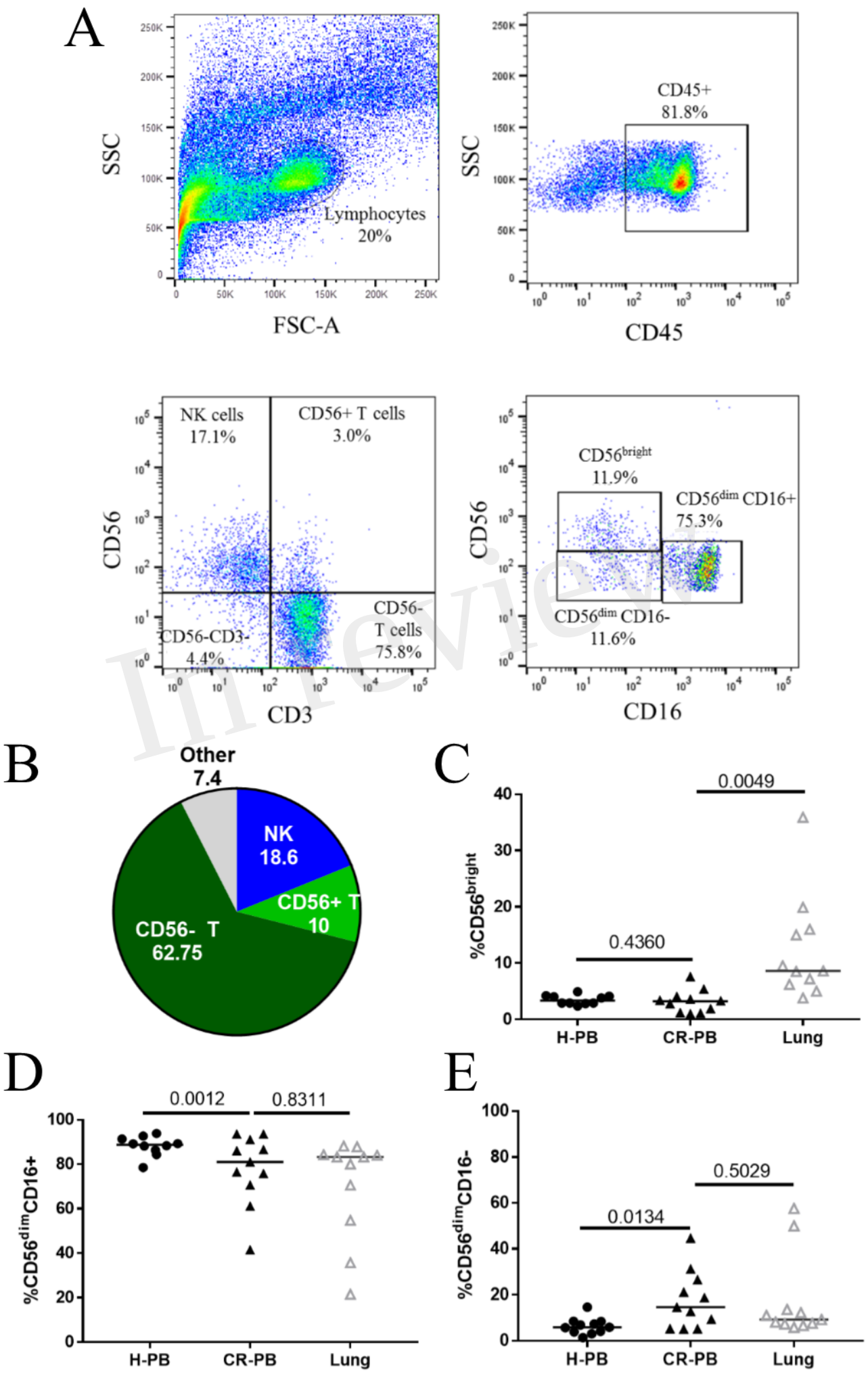
A
SSC
FSC-A
Lymphocytes
20%
CD45+
81.8%
CD45
NK cells
17.1%
CD56+ T cells
3.0%
CD56-
T cells
75.8%
CD56-CD3-
4.4%
CD3
CD56bright
11.9%
CD56dim CD16+
75.3%
CD56dim CD16-
11.6%
CD16
B
Other
7.4
NK
18.6
CD56+ T
10
CD56- T
62.75
C
%CD56bright
0.0049
0.4360
H-PB
CR-PB
Lung
D
%CD56dimCD16+
0.0012
0.8311
H-PB
CR-PB
Lung
E
%CD56dimCD16-
0.0134
0.5029
H-PB
CR-PB
Lung

Figure 2.TIF

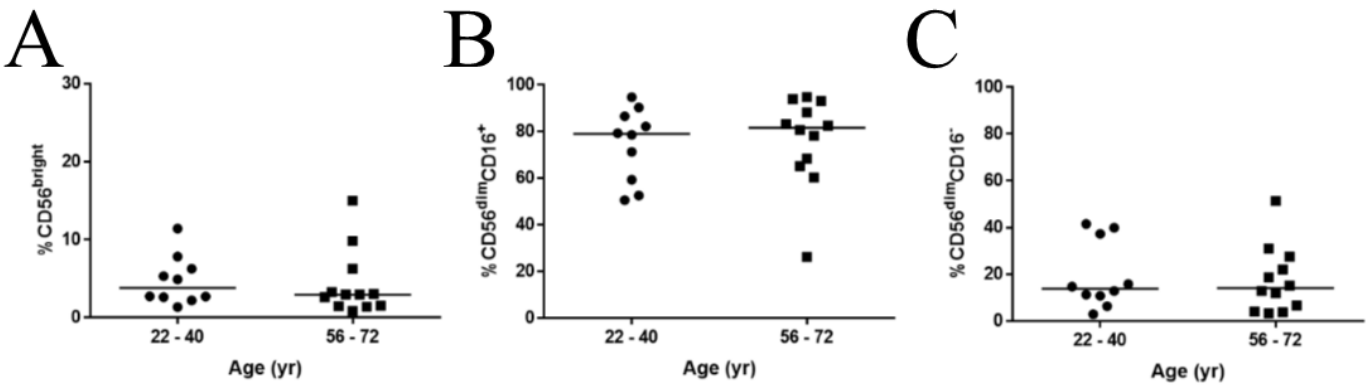

Figure 3.TIF

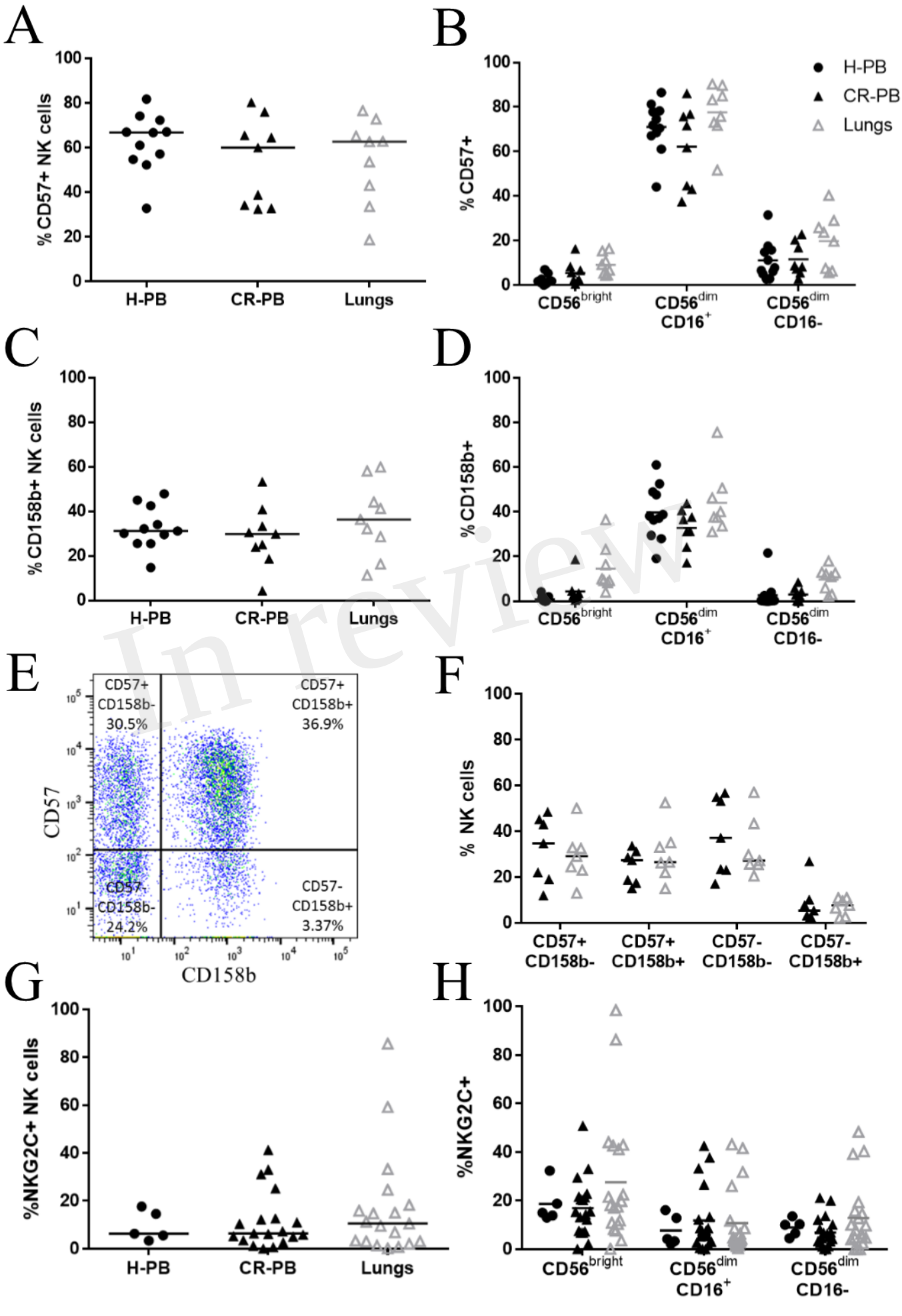

Figure 4.TIF

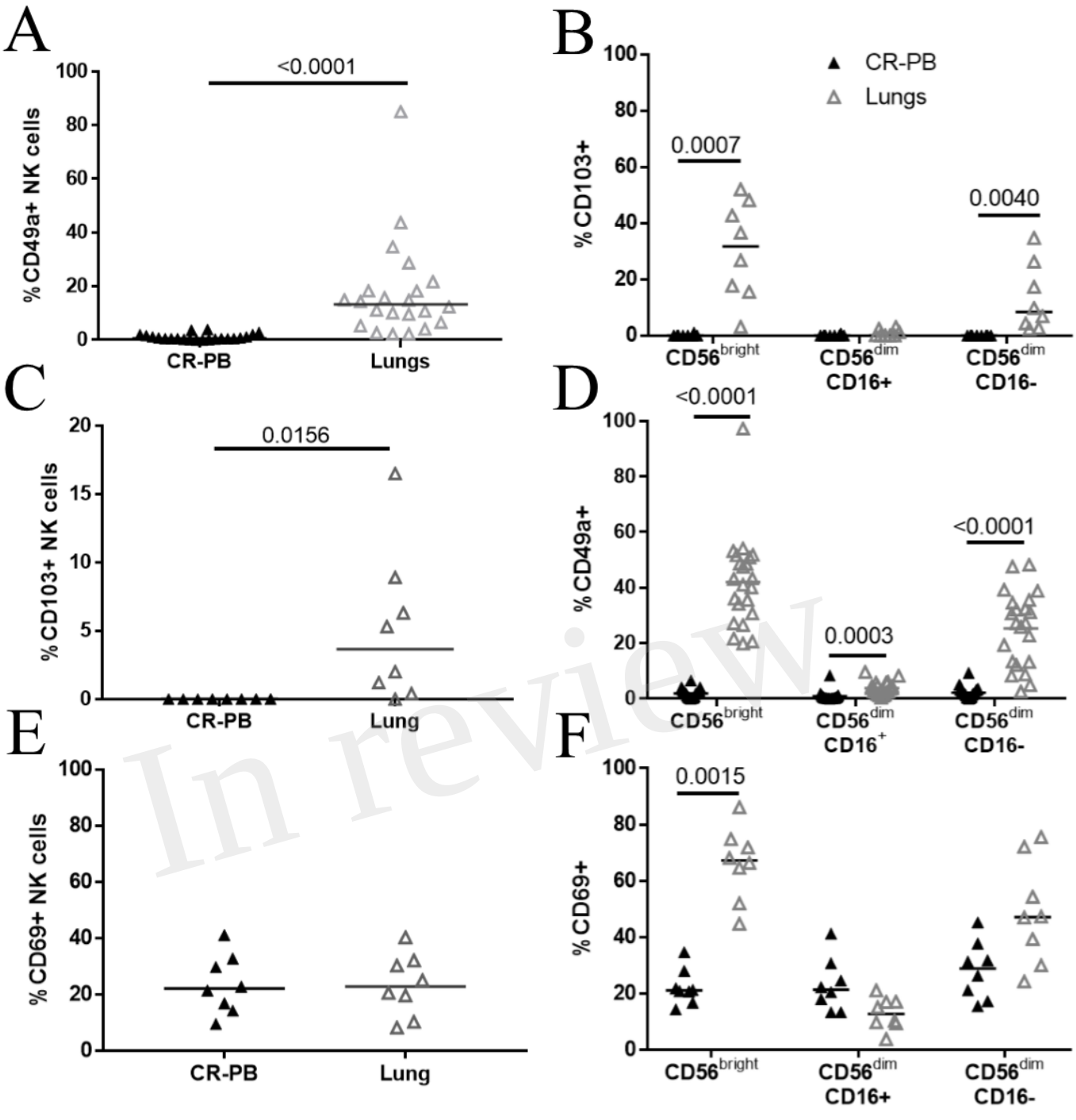

Figure 5.TIF

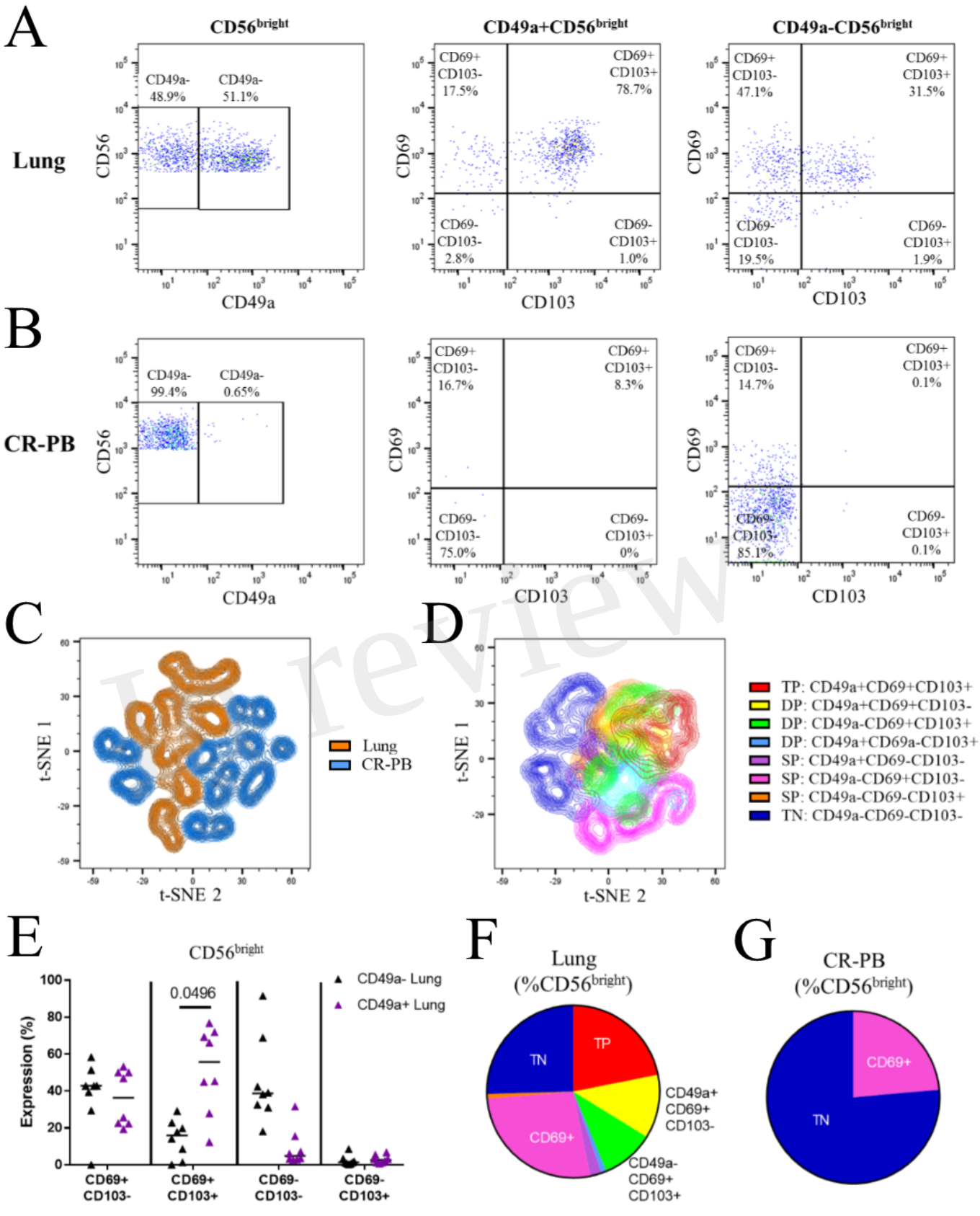
A
CD56bright
CD49a+CD56bright
CD49a-CD56bright
Lung
CD49a- 48.9%
CD49a- 51.1%
CD56
CD49a
CD69+ CD103- 17.5%
CD69+ CD103+ 78.7%
CD69- CD103- 2.8%
CD69- CD103+ 1.0%
CD69
CD103
CD69+ CD103- 47.1%
CD69+ CD103+ 31.5%
CD69- CD103- 19.5%
CD69- CD103+ 1.9%
B
CR-PB
CD49a- 99.4%
CD49a- 0.65%
CD69+ CD103- 16.7%
CD69+ CD103+ 8.3%
CD69- CD103- 75.0%
CD69- CD103+ 0%
CD69+ CD103- 14.7%
CD69+ CD103+ 0.1%
CD69- CD103- 85.1%
CD69- CD103+ 0.1%
C
t-SNE 1
t-SNE 2
Lung
CR-PB
D
TP: CD49a+CD69+CD103+
DP: CD49a+CD69+CD103-
DP: CD49a-CD69+CD103+
DP: CD49a+CD69a-CD103+
SP: CD49a+CD69-CD103-
SP: CD49a-CD69+CD103-
SP: CD49a-CD69-CD103+
TN: CD49a-CD69-CD103-
E
CD56bright
Expression (%)
0.0496
CD49a- Lung
CD49a+ Lung
CD69+ CD103-
CD69+ CD103+
CD69- CD103-
CD69- CD103+
F
Lung (%CD56bright)
TP
TN
CD69+
CD49a+ CD69+ CD103-
CD49a- CD69+ CD103+
G
CR-PB (%CD56bright)
CD69+
TN

Figure 6.TIF

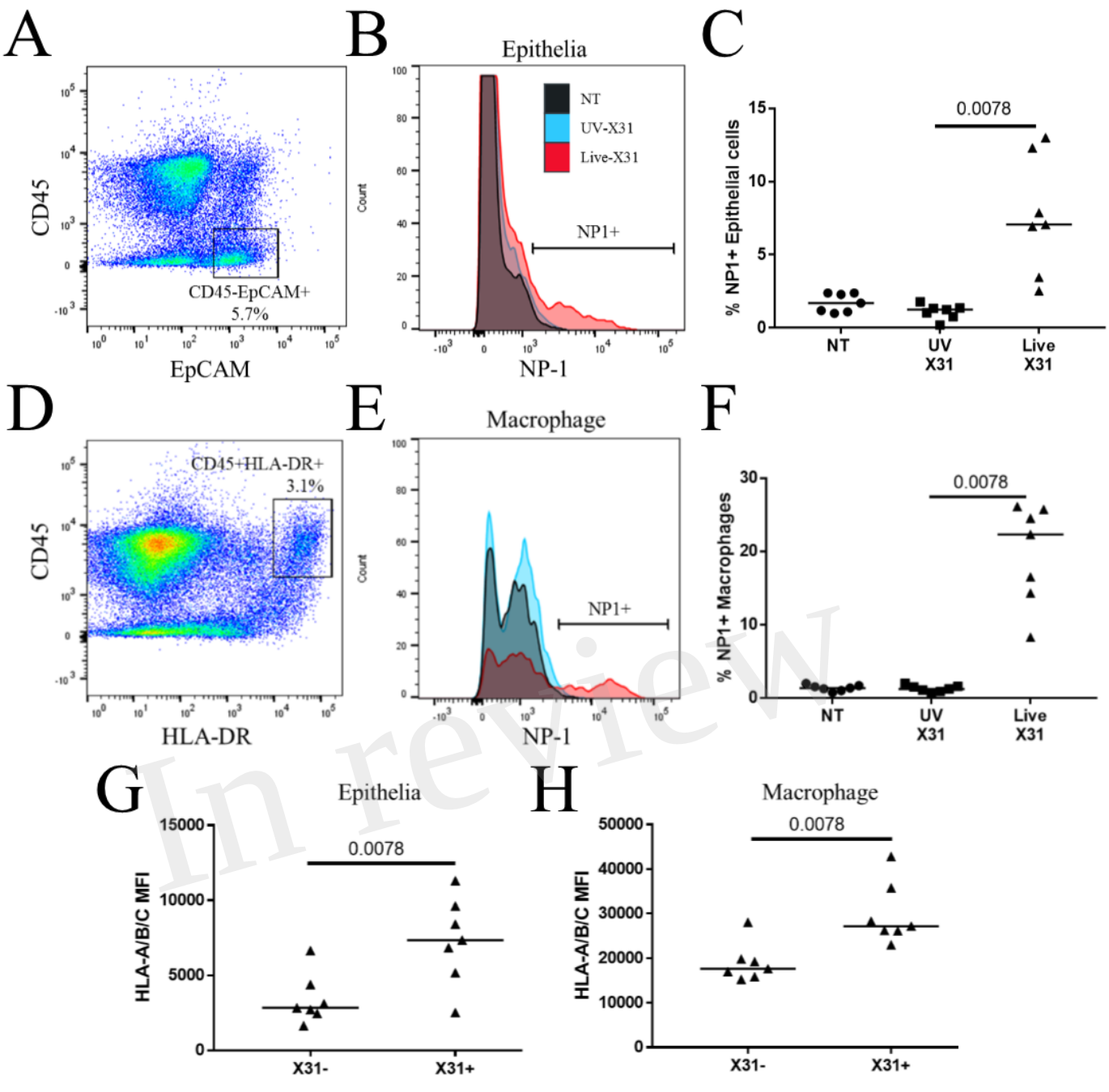

Figure 7.TIF

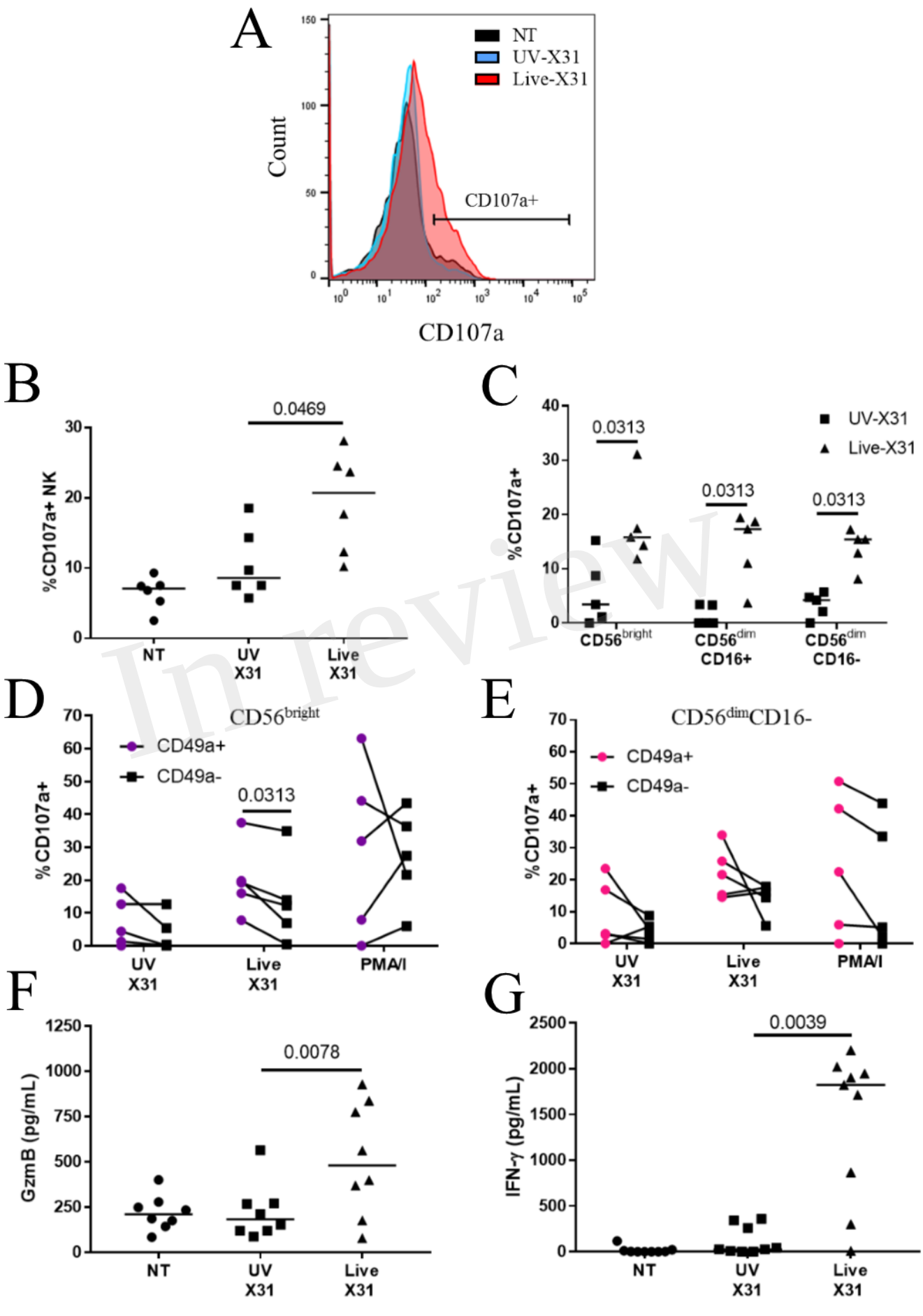

Figure 8.TIF

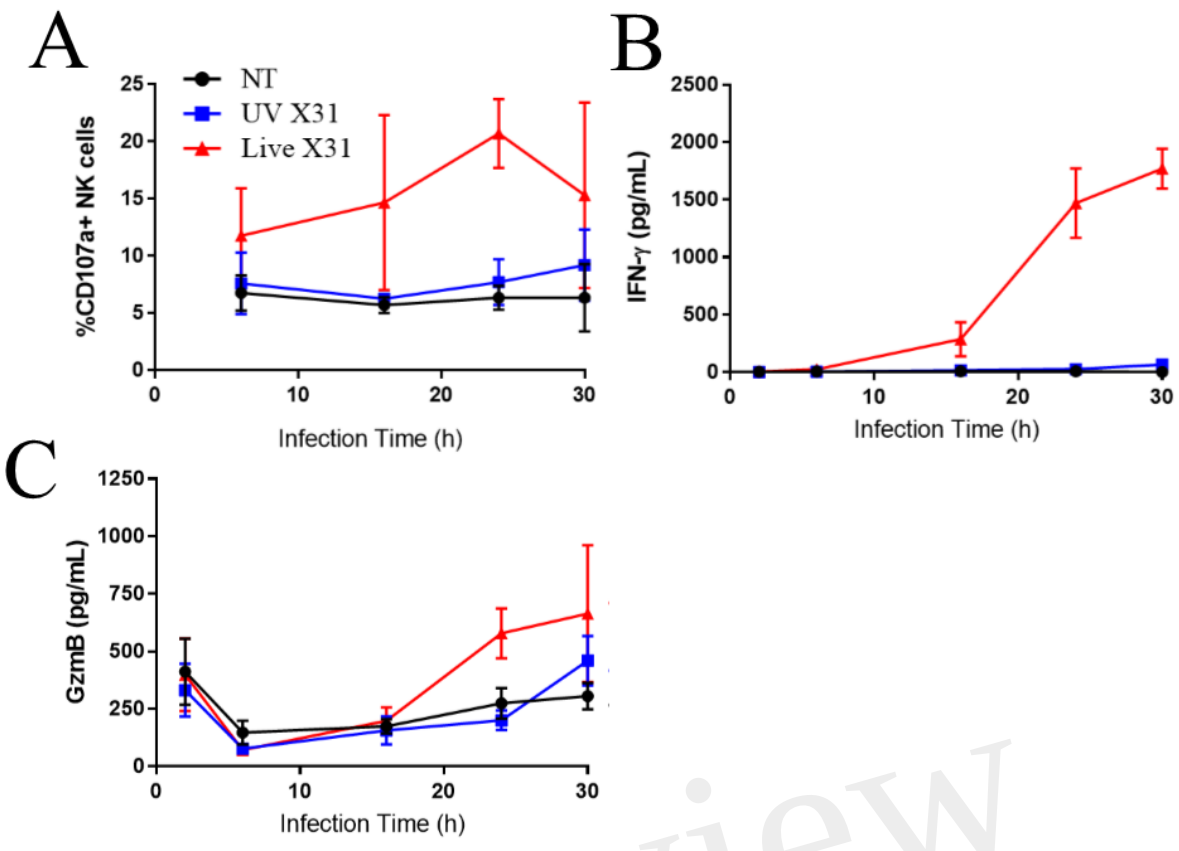

Figure 9.TIF

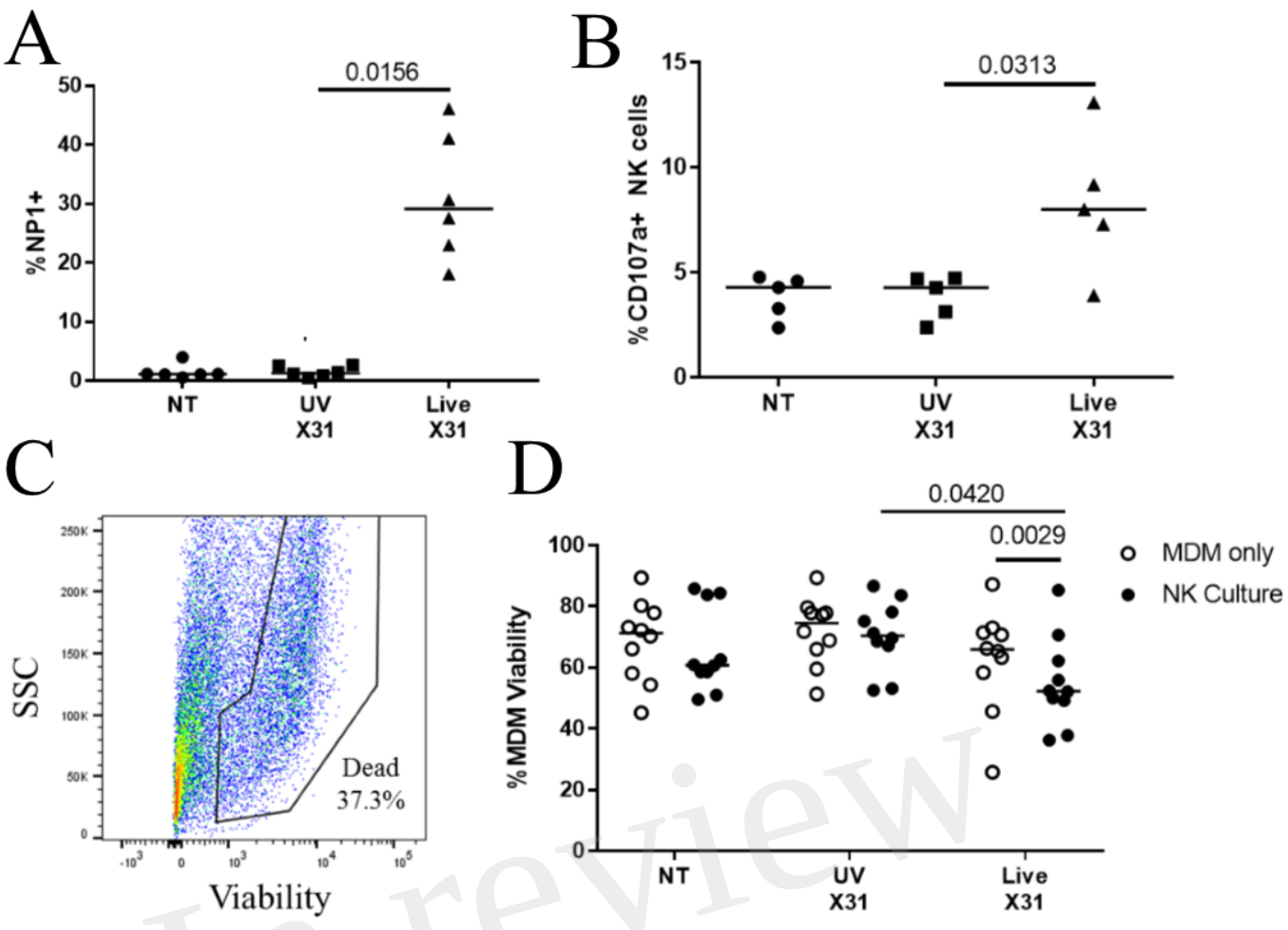

Figure 10.TIF

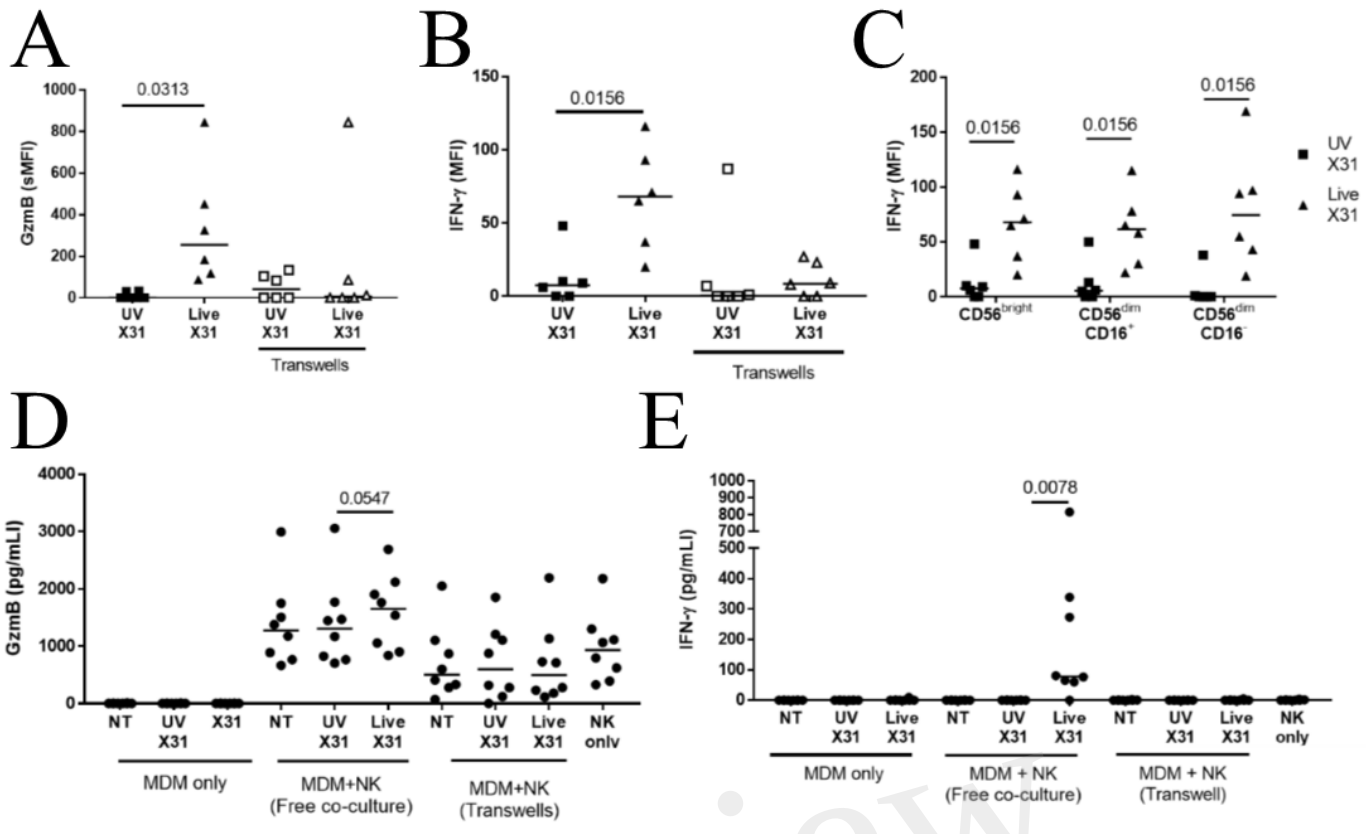

Figure 11.TIF